THE STAR FORMATION LAW IN GALACTIC DISKS

ROBERT C. KENNICUTT, JR.[1]
Steward Observatory, University of Arizona
Received 1988 November 29; accepted 1989 February 23

ABSTRACT

Measurements of the distribution of Hα emission in galaxies have been combined with published H I and CO data, in order to reassess the dependence of the massive star formation rate (SFR) on the density and dynamics of the interstellar gas. The disk-averaged Hα surface brightness is correlated with the mean atomic and total gas surface densities, but is only weakly correlated with the mean molecular gas density inferred from CO emission. Radial profiles of gas and Hα emission in 15 galaxies have been used to define the relationship between the SFR and gas surface density. In dense regions the SFR and total gas density are well represented by a Schmidt power-law relation ($R = a\Sigma_g^N$), with index $N = 1.3 \pm 0.3$, and nearly the same value for the zero point a, at least for the galaxies in our sample. This Schmidt law breaks down, however, at densities below a critical threshold value. Massive star formation is completely suppressed at surface densities well below the threshold, while at densities near the the threshold value the slope of the SFR–density relation is much steeper than a normal Schmidt law. The observed threshold densities vary by an order of magnitude among the galaxies in our sample and appear to be largely independent of whether the predominant gas phase is atomic or molecular. The star formation threshold appears to be associated with the onset of large-scale gravitational instabilities in the gas disks. A simple single-fluid (Toomre) disk stability model predicts threshold densities and radii which are in excellent agreement with the observations. The same analysis demonstrates that the radial distribution of gas in late-type galaxies closely follows the threshold surface density, confirming a hypothesis originally proposed by Quirk, and indicating the importance of star formation thresholds in virtually all parts of the disk. The combination of a nearly linear star formation law at high densities with a strongly nonlinear SFR–density law near the threshold redresses many of the previous observational difficulties with the Schmidt law and may provide physical insights into such diverse phenomena as nuclear and disk starbursts, the suppression of star formation in gas-rich S0 galaxies and low surface brightness galaxies, star formation in spiral arms, the observation of radial cutoffs to stellar disks, and the star formation histories of disk galaxies.

Subject headings: galaxies: evolution — galaxies: stellar content — stars: formation

I. INTRODUCTION

An important problem in galactic structure and evolution is the relationship between the large-scale star formation rate (SFR) and the physical properties of the interstellar gas. Simple parametrizations between the SFR and the density or other properties of the gas form the foundation for most models of the chemical and luminosity evolution of galaxies, and for many models of galaxy formation. Unfortunately our understanding of the star formation process on galactic scales is still at a primitive stage. Most current galactic evolution models, for example, are still based on the simple parametrization of Schmidt (1959), wherein the SFR is assumed to depend only on the local gas density, according to a simple power law:

$$R = a\rho_g^n, \tag{1}$$

usually with $n = 1$–2. Over the past 30 years this "Schmidt law" has been used almost exclusively to describe the large-scale behavior of star formation in galaxies, and, although its validity has been frequently challenged, the available data on star formation in galaxies have not provided a clear alternative.

Previous attempts to measure the form of the Schmidt law,

mostly based on comparisons of surface densities of blue stars of H II regions with gas surface densities, have confirmed the presence of a density–SFR correlation (e.g., Berkhuijsen 1977; Freedman 1984, and references therein), but the derived values of the best fitting power-law slopes show a large dispersion, with $0 < n < 4$. Part of this dispersion may be caused by extraneous factors such as resolution smearing effects (Freedman 1984), differences in the methods used to measure the SFR (Madore 1977), or the neglect of atomic or molecular gas (Talbot 1980), but large variations in n are observed even when identical techniques are applied to different parts of the same galaxy (e.g., Madore, van den Bergh, and Rogstad 1974; Freedman 1984), suggesting that the star formation law does not have a universal form or slope.

Several other general observations are also difficult to reconcile with a universal Schmidt law. For example, the relatively slow evolution of the stellar birthrate in galactic disks argues for a very weak ($n \ll 1$) dependence of the global SFR on gas density (Miller and Scalo 1979; Twarog 1980; Kennicutt 1983, 1986). The relatively weak dependence of the SFR on CO emission also implies $n < 1$ (Lord 1987, and references therein). On the other hand, a very nonlinear SFR–density dependence ($n \gg 2$) is required to explain other observations. For example, many interesting galaxies exhibit order-of-magnitude increases in global SFRs with only modest increases in gas surface density (Bushouse 1987; Kennicutt *et al.* 1987). Likewise, in many spiral galaxies the star formation is strongly concen-

trated to the arms, while the gas density is only mildly enhanced in the arms (Lord 1987). At the other extreme, many S0 and Sa galaxies contain substantial gas disks but virtually no current star formation (Schommer and Bothun 1983; van Driel 1987); similar low-level star formation thresholds have been observed in the outer regions of spiral and irregular galaxies (Skillman 1987; Guideroni 1987). Although some of these observations could be explained by invoking Schmidt laws with either very low or very high values for the power-law index *n*, a single power law clearly cannot account for all of the phenomena. These problems have led many workers to propose modifications to the Schmidt law or new star formation laws altogether (e.g., Talbot and Arnett 1975; Dopita 1985; Wyse 1986; Silk 1987), and have led some to question whether a global law exists at all (e.g., Hunter and Gallagher 1986).

This paper reports the first results of a comprehensive reinvestigation of the regulation of the large-scale star formation rate in disk galaxies. The goals of the project are twofold. The first is to improve the empirical analysis of the SFR versus gas density law over previous studies, by using a quantitative star formation tracer, Hα surface brightness, to compare the star formation laws in different galaxies on a common absolute scale, and correlating the resulting SFRs with the atomic, molecular, and total gas densities. The combination of the new Hα data with several recently published surveys of H I and CO emission in galaxies allows us to study the behavior of the star formation law over a much larger range of gas densities and star formation environments than had been possible previously. The second objective is to use the observations to isolate the principal physical mechanisms which regulate the SFR, in hopes of eventually supplanting the Schmidt parametrization with a physically based star formation law.

This paper is concerned with the behavior of the star formation law on large scales, averaged over entire disks, and averaged as a function of galactocentric radius. The data are described in § II, and the observed SFR versus density relations are discussed in § III. In § IV we compare the observed star formation laws with what would be expected from simple gravitational stability considerations and reintroduce a rudimentary threshold model for the star formation and gas distributions (Quirk 1972). We discuss the physical nature of the star formation law in § V, and its implications for several general problems in § VI. Future papers will deal with the star formation law on smaller scales, and with the regulation of the SFR at high gas densities, where other physical mechanisms may be important.

II. DATA

Although the Schmidt law was. originally formulated in terms of the volume densities of young stars and gas, the principal observable quantities are the projected surface densities of gas and star formation. In this case the law takes the form we shall be concerned with here:

$$\Sigma_{\text{SFR}} = a\Sigma_g^N , \qquad (2)$$

with an upper case *N* to distinguish the power-law index from the coefficient in equation (1). Note that for a nearly linear star formation law ($n \approx 1$), $N \approx n$.

We have analyzed the star formation properties of two samples of galaxies. Spatially resolved data on the distributions of Hα, H I, and CO emission are available in common for 15 galaxies, and these have been used to study the radial dis-

tribution of the gas and young stars, and the form of the star formation law averaged over kiloparsec scales. In addition, data on the integrated Hα fluxes and average H I and/or H$_2$ surface densities are available for a larger sample of galaxies, and these will be used to investigate whether there is a meaningful global star formation law.

a) H I and CO Data

H I distributions were taken from the 21 cm studies of Rogstad and Shostak (1972), Huchtmeier and Witzel (1979), Newton (1980), Bosma (1981), Bosma, Goss, and Allen (1981), Wevers, van der Kruit, and Allen (1986), Tacconi and Young (1986), and Warmels (1986, 1988). The radial H I profiles, corrected to face-on orientation, were derived from complete aperture synthesis observations, except for a few galaxies in the Warmels survey, where partial observations along one or more "resolution axes" were obtained.

Data on the distributions of molecular gas were taken from the CO surveys of Young and Scoville (1982a, c), Scoville and Young (1983), Solomon et al. (1983), Garman and Young (1986), Tacconi and Young (1986), Lord (1987), Young (1987), and Kenney and Young (1988a). Most of these observations consist of strip scans, usually along the major axis, with a resolution of 45"–50", corresponding to a linear resolution of 1–5 kpc for the galaxies in our sample. We have followed the convention in these papers and assumed a constant conversion between CO intensity and H$_2$ column density. Since a variety of conversion factors were used in the original studies, it was necessary to reconvert the column densities to a common scale. Following Bloemen et al. (1986) and Kenney (1987), we adopted

$$N(\text{H}_2 \text{ cm}^{-2}) = 2.8 \times 10^{20} I_{\text{CO}} \cos i (\text{K km s}^{-1}) . \qquad (3)$$

It is possible that this conversion factor varies substantially within the galaxies in our sample (Bloemen et al. 1986; Maloney 1987), and this uncertainty, along with extinction effects at Hα, is probably the main source of systematic error in this study.

The azimuthally averaged radial distributions of H I and H$_2$ density were combined to derive a total gas surface density distribution. In general, the CO measurements do not extend as far in radius as the H I data, and in order to avoid introducing an artificial feature in the gas distributions we extrapolated the CO intensity, using an exponential fit to the observed data points (and upper limits). In most cases the radial gradient in CO emission was sufficiently steep that the molecular gas made only a small contribution to the total gas density in the regions in question.

The same data were used to construct a rotation curve for each galaxy, for modeling the dynamics and gravitational stability of the disks. Both the CO and H I data were used to derive a composite rotation curve, since they provide complementary information on the gas kinematics in the inner and outer disks, respectively). In most galaxies the rotation curves could be fitted to a flat curve in the outer regions and a linearly rising inner portion, and this approximate form was used in the subsequent modeling.

For the comparison of integrated SFRs and gas densities we used the compilation of average H I surface densities in Warmels (1986) and compilations of average H$_2$ densities in Stark, Elmegreen, and Chance (1987) and Kenney (1987). The H I densities were derived directly from fully sampled maps, so they should accurately represent the mean values in the star-

forming disks. The densities were averaged within a radius equal to half of the optical radius (25 mag arcsec^{-2}), in order to minimize any effects of gas stripping in the outer parts of the Virgo cluster members. Most of the CO data are "interpolated fluxes," derived from measurements at one or more positions along a single axis, and averaged assuming a functional form for the CO radial distribution. These fluxes were converted to H$_2$ surface densities using equation (3) and are averaged within the optical radius (25 mag arcsec^{-2}), as listed by de Vaucouleurs, de Vaucouleurs, and Corwin (1976).

b) Hα Data

We chose Hα emission as the primary star formation tracer, because the Hα flux is directly proportional to the massive ($\geq 10\ M_\odot$) SFR, and, in cases where photometry is available, one can compare the SFR distributions in different galaxies on a common absolute scale. The Hα fluxes can be converted to approximate SFRs using the equations given by Kennicutt (1983, 1988), but in this paper only the observed Hα and H II region distributions will be used.

Integrated Hα + [N II] fluxes are available for 63 galaxies with H I and CO data (Kennicutt and Kent 1983; Kennicutt et al. 1987). These were converted to net Hα fluxes using the average [N II]/Hα ratios provided in Kennicutt and Kent (1983). The fluxes have been corrected for foreground Galactic extinction, but not for extinction within the galaxies themselves, for reasons discussed below. A mean Hα surface brightness was also calculated for each galaxy, by dividing the total flux by the area of the disk, using the corrected optical diameters listed in de Vaucouleurs, de Vaucouleurs, and Corwin (1976).

Radial distributions of Hα emission were measured for 15 galaxies with well-determined H I and CO distributions. The primary source of these data is a set of calibrated Hα and continuum images obtained with the Carnegie direct image-tube camera on the Kitt Peak National Observatory 2.1 m and No. 1 0.9 m telescopes. The main advantage of this instrument is its large field, 7′ and 15′ on the 2.1 m and 0.9 m telescopes, respectively, an important consideration because most of the program galaxies possess diameters in this range. Each galaxy was imaged behind an interference filter centered on redshifted Hα (FWHM = 20–38 Å), providing excellent isolation of the disk H II regions, and with a 100 Å wide continuum filter centered at 6400 or 5100 Å. Calibration of the intensity scales was accomplished using sensitometer exposures and photoelectric observations of selected H II regions in each field from Kennicutt (1988). Details of the observation and calibration procedures are described in Kennicutt, Edgar, and Hodge (1989), and reproductions of many of the images have been published by Hodge and Kennicutt (1983a, c).

Two methods were used to derive the radial distribution of the Hα emission. The most direct approach, areal surface photometry of the Hα maps, proved to be impractical for most of the galaxies, due to a low-level scattered light background in the image tube which was not completely removed by the flat-field calibration. Instead we used the distributions of the resolved H II regions to derive approximate radial Hα profiles. For six galaxies (M33, M51, M101, NGC 2403, NGC 2841, NGC 4736) with complete H II region photometry (Kennicutt, Edgar, and Hodge 1989), the radial profile was derived by summing the H II region fluxes in elliptical annuli. This procedure was especially well suited to late-type spirals, which comprise most of our sample, because almost all of their total

Hα emission is produced by the detected H II regions (Kennicutt, Edgar, and Hodge 1989).

For galaxies where complete photometry was not available, the approximate Hα profile was derived from the unweighted H II region surface density distribution, calibrated in surface brightness using the total Hα flux (Kennicutt and Kent (1983). As long as the H II region luminosity function is not a strong function of radius, this normalized H II region profile should provide an excellent approximation to the distribution of Hα brightness. This was tested by comparing the flux-weighted and unweighted H II region profiles in cases where complete H II region photometry was available; Figure 1 shows such comparison for M101, an active star forming Sc galaxy, and NGC 2841, an early Sb galaxy with a much lower SFR. In most galaxies the H II region distributions trace the Hα profiles to better than ±30%, over a range of 2–3 orders of magnitude in surface brightness. This is consistent with independent data which indicate that the H II region luminosity function does not vary strongly with galactocentric radius (Kennicutt, Edgar, and Hodge 1989). M101 is one of the most discrepant cases (see Fig. 1), with local deviations of up to ±50% in the main star-forming disk (caused by unusually bright H II regions), and a larger deviation in the outermost disk, where only a few faint H II regions are present. This comparison demonstrates that photometrically measured profiles are required to study the detailed behavior of the star formation distribution in disk galaxies, but the H II region profiles provide reliable information on the gross shapes and radial extents of the SFR distributions and are quite adequate for the purposes of this paper. We are currently using CCD imagers to obtain deep Hα surface photometry for many of these galaxies, and these data will be published in a future paper.

The largest source of systematic error in the interpretation of the Hα distributions is extinction. Individual H II regions in these galaxies suffer typical extinctions at Hα of 0.5–2 mag (e.g., Israel and Kennicutt 1980; McCall, Rybski, and Shields 1985;

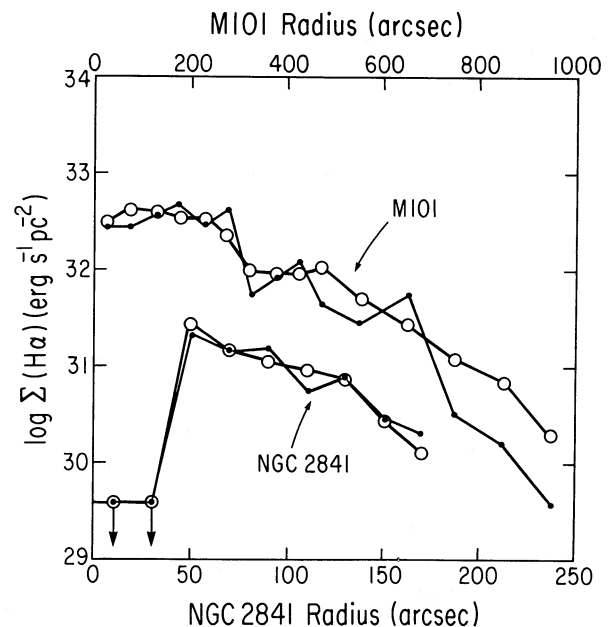
FIG. 1.—Comparison of Hα surface brightness profiles in M101 and NGC 2841, derived from summing the fluxes of the resolved H II regions (solid points), and as estimated from the unweighted number densities of H II regions (open circles).

van der Hulst *et al.* 1988), and this clearly must be taken into account if the Hα fluxes are to be used to estimate absolute star formation rates. The studies cited above indicate that the extinction in H II regions does not vary strongly with radius, except possibly in the very inner disks ($R = 0$–2 kpc) of some galaxies, where the extinction can be considerably higher than average. Consequently, we chose to use the uncorrected Hα surface brightness profiles but excluded the innermost regions from the analysis.

The Hα emission distributions for the 15 main program galaxies are shown in Figure 2. In addition, we have used the uncalibrated radial distributions of H II regions in several other galaxies (M81, NGC 628, 925, 2366, 4548, 4569, 4647, 5055, 5962, 7331) in order to derive the scale lengths and radial extents of the H II region disks. The latter data were taken from Hodge (1974) and Hodge and Kennicutt (1983*b*).

Table 1 summarizes the properties and sources of data for the galaxies with spatially resolved H I, CO, and Hα data. The table also lists 7 other spirals and five S0 galaxies with published H I and CO distributions (but no Hα data), which were used to study the stability properties of the interstellar gas

(§§ IV, VI). Table 2 lists the average H I, CO, and Hα surface densities for the 63 galaxies with integrated measurements.

III. RESULTS

a) Integrated Properties

A question which is especially relevant for galaxy evolution modeling is whether the total SFR in a galaxy is correlated with its average gas content. Several investigators have pointed out that the total Hα, ultraviolet, and far-infrared luminosities of galaxies are linearly correlated with their total CO luminosity and/or H I mass, but the physical significance of these correlations is questionable. The range in galaxy mass and luminosity in most samples is usually much larger than the range of gas or SFR densities, so the apparently tight linear correlations between total SFR and total gas mass are predominantly artifacts of scaling, rather than meaningful physical relationships (see Stark *et al.* 1986). This problem can be avoided by comparing SFRs and gas masses which are normalized to the total luminosity or size of the parent galaxies.

Figures 3*a*–3*c* show the relationships between the mean Hα

TABLE 1

GALAXIES WITH GAS AND Hα DISTRIBUTIONS

			SOURCES		
GALAXY	TYPE	DISTANCE (Mpc)	H I Data	CO Data	Hα Data
NGC 598 (M33)	Sc	0.8	1	10	17
NGC 628	Sc	10.	2		19
NGC 925	Sc	9.5	2		19
NGC 2366	Sc	3.5	2		19
NGC 2403	Sc	3.5	2	10	17
NGC 2841	Sb	12.	3	11	17
NGC 4254	Sc	17.5	4	12	18
NGC 4303	Sc	17.5	4	12	18
NGC 4321	Sc	17.5	4	12	18
NGC 4535	Sc	17.5	4	12	18
NGC 4548	SBb	17.5	4	12	20
NGC 4569	Sab	17.5	4	12	20
NGC 4571	Sc	17.5	4	12	18
NGC 4647	Sc	17.5	4	12	21
NGC 4654	Sc	17.5	4	12	18
NGC 4689	Sc	17.5	4	12	18
NGC 4736	Sab	4.5	3	13	17
NGC 5194 (M51)	Sbc	7.5	5	14	17
NGC 5457 (M101)	Sc	6.	6, 7	15	17
NGC 6946	Sc	5.	8	16	18
NGC 7331	Sb	14.	3	11	19
NGC 3941	SB0/a	20.	9		
NGC 4192	Sb:	17.5	4	12	
NGC 4203	S0	23.	9		
NGC 4216	Sb	17.5	4	12	
NGC 4262	SB0	17.5	9		
NGC 4388	Sab	17.5	4	12	
NGC 4394	SBb	17.5	4	12	
NGC 4579	Sab	17.5	4	12	
NGC 4639	SBb	17.5	4	12	
NGC 4698	Sa	17.5	4	12	
NGC 5101	SB0/a	28.	9		
NGC 5102	S0	20.	9		

NOTES.—Sources of data as follows: (1) Newton 1980. (2) Wevers, van der Kruit, and Allen 1986. (3) Bosma 1981. (4) Warmels 1988. (5) Rogstad and Shostak 1972. (6) Huchtmeier and Witzel 1979. (7) Bosma, Goss, and Allen 1981. (8) Tacconi and Young 1986. (9) van Driel 1987. (10) Young 1986. (11) Young and Scoville 1982*c*. (12) Kenney and Young 1988. (13) Garman and Young 1986. (14) Scoville and Young 1983. (15) Solomon *et al.* 1983. (16) Young and Scoville 1982*a*. (17) H II region photometry; this paper. (18) Calibrated H II region number densities; this paper. (19) Hodge and Kennicutt 1983*b*. (20) Hodge 1974. (21) Kennicutt *et al.* 1987.

TABLE 2

AVERAGE SURFACE DENSITIES AND SURFACE BRIGHTNESSES

Galaxy	$\Sigma(H\,\text{I})$ ($M_\odot$ pc^{-2})	$\Sigma(H_2)$ ($M_\odot$ pc^{-2})	$\Sigma(H\alpha)$ (10^{32} ergs s^{-1} pc^{-2})
NGC 157	...	12.4	4.8
NGC 628	5.2	...	4.0
NGC 1058	3.8	1.8	2.4
NGC 1073	7.6	...	1.4
NGC 1291	0.1	...	<0.2
NGC 2841	1.3	3.4	0.1
NGC 2976	...	4.0	4.3
NGC 3169	...	9.6	<1
NGC 3368	3.8	...	1.2
NGC 3504	...	38.7	8.1
NGC 3631	...	5.9	3.8
NGC 3726	6.7	...	1.8
NGC 3810	...	16.2	5.2
NGC 3938	6.6	9.4	2.9
NGC 4152	11.5	6.1	5.1
NGC 4178	9.8	0.9	2.1
NGC 4189	9.5	4.9	3.2
NGC 4212	...	11.2	4.1
NGC 4237	...	24.8	1.1
NGC 4254	7.5	16.3	7.8
NGC 4293	...	1.6	<1
NGC 4294	9.5	<1.5	5.6
NGC 4298	...	12.8	2.0
NGC 4299	13.4	...	12.3
NGC 4303	6.5	8.2	7.2
NGC 4321	4.4	13.9	3.4
NGC 4394	2.0	2.6	<1
NGC 4501	3.5	14.2	1.5
NGC 4526	...	<0.4	<0.5
NGC 4535	2.7	7.7	1.6
NGC 4536	...	2.4	1.3
NGC 4548	0.9	2.8	0.6
NGC 4561	34.2	...	4.1
NGC 4567	...	13.5	1.9
NGC 4568	...	16.5	2.4
NGC 4569	1.0	7.9	0.7
NGC 4571	2.9	4.4	1.2
NGC 4579	1.9	5.2	<1
NGC 4594	0.4	...	<0.3
NGC 4631	...	8.5	2.9
NGC 4647	4.7	35.4	3.4
NGC 4651	6.3	4.1	4.2
NGC 4654	7.0	8.5	2.8
NGC 4689	2.3	5.1	1.7
NGC 4713	9.3	<1.8	8.3
NGC 4736	3.2	5.1	2.4
NGC 4775	12.0	...	7.8
NGC 4808	...	1.8	8.0
NGC 4826	0.3	6.5	1.3
NGC 4866	...	<0.7	<0.5
NGC 4900	7.2	...	10.3
NGC 5033	6.3	3.7	0.9
NGC 5055	7.3	...	2.2
NGC 5194	6.8	27.4	5.7
NGC 5364	...	5.4	1.3
NGC 5474	...	1.5	1.5
NGC 6217	5.4	...	4.8
NGC 6412	...	1.5	3.2
NGC 6503	5.1	...	3.7
NGC 6643	...	16.0	4.5
NGC 6946	8.8	24.9	4.2
NGC 7217	...	4.5	2.2
NGC 7742	...	7.0	3.9

surface brightness (proportional to the SFR per unit area, Σ_{SFR}) and the average H I, H$_2$, and total H surface densities. The lines show the trends expected for Schmidt laws with $N = 1$ and 2. The average SFR is most strongly correlated with H I and total gas surface densities (see Guiderdoni and Rocca-

Volmerange (1985) and Donas et al. (1987). The best fitting power laws lie in the range $N \approx 1.2–1.6$, but the samples are small and most of the galaxies lie within a relatively narrow range in densities, so one should be cautious in interpreting this result. Part of the dispersion in these relations may be due to variations in extinction at Hα, but most of the scatter appears to be real.

The most puzzling result in Figure 3 is the absence of any significant correlation between the Hα emission and the surface density of molecular gas, as depicted in Figure 3c. This contradicts earlier claims of a tight linear correlation between global CO emission and the SFR (e.g., Young and Scoville 1982b; Young, Scoville, and Brady 1985; Tacconi and Young 1987), all based on comparisons of total luminosities and masses; this demonstrates the importance of comparing luminosity and mass-independent parameters when testing for physical relationships between the SFR and gas content. Buat, Deharveng, and Donas (1989) draw similar conclusions from a comparison of UV, H I, and CO data.

Before attempting to interpret this result, it is pertinent to consider whether problems with the CO or Hα observations could be responsible for the scatter in Figure 3c. Errors in the CO fluxes could be responsible for a few of the most discrepant points, but they cannot account for most of the general dispersion. The published H$_2$ masses and densities were extrapolated from CO measurements which only partially sample the disks, and small errors in the assumed profile shape can lead to significant errors in the integrated flux. Comparisons of the fluxes listed for galaxies in common by Kenney and Young (1988) and Stark, Elmegreen, and Chance (1987) show a few objects with disagreements as large as a factor of 5, which presumably reflects this problem, but most of the fluxes agree to within ±30%. If the comparison in Figure 3c is restricted to galaxies for which full major axis scans are available, the correlation is slightly improved, but the scatter is still very large. Thus, while errors in the CO or Hα flux probably contribute to the scatter in Figure 3c, most of the dispersion appears to be real.

Extinction is probably the most significant source of error in the Hα data. As discussed earlier, variations of as much as 1–2 mag in extinction could be present in the sample, and the galaxies with the highest molecular gas contents might well suffer the highest extinction, introducing an artificial scatter into Figure 3c. It seems unlikely, however, that this effect can be the major source of dispersion. If extinction were the sole problem, for example, we would not observe such strong correlations between Hα emission and the H I and total gas densities. Furthermore, comparisons of CO emission with other types of star formation tracers, such as far-infrared (FIR) emission, show a large dispersion as well (Stark et al. 1986; Kenney 1987; Pompea and Rieke 1989). This is illustrated in Figure 3d, which shows the relation between FIR (40–300 μm) surface brightness and H$_2$ surface density, using IRAS fluxes compiled by Kenney (1987) and Kennicutt et al. (1987). The correlation here is somewhat better than in Figure 3c, suggesting that extinction effects at Hα may indeed be significant, but the scatter is still much larger than in Figures 3a–3b.

In order to place these results on a more formal footing, we constructed a statistical sample of 27 spiral galaxies in Table 2 for which complete H I, CO, Hα, and FIR data are available, and computed Spearman rank correlation coefficients for Hα and FIR surface brightness versus each of the three gas surface densities. The results of such a comparison are relatively insensitive to the form of the correlation test, but they are somewhat
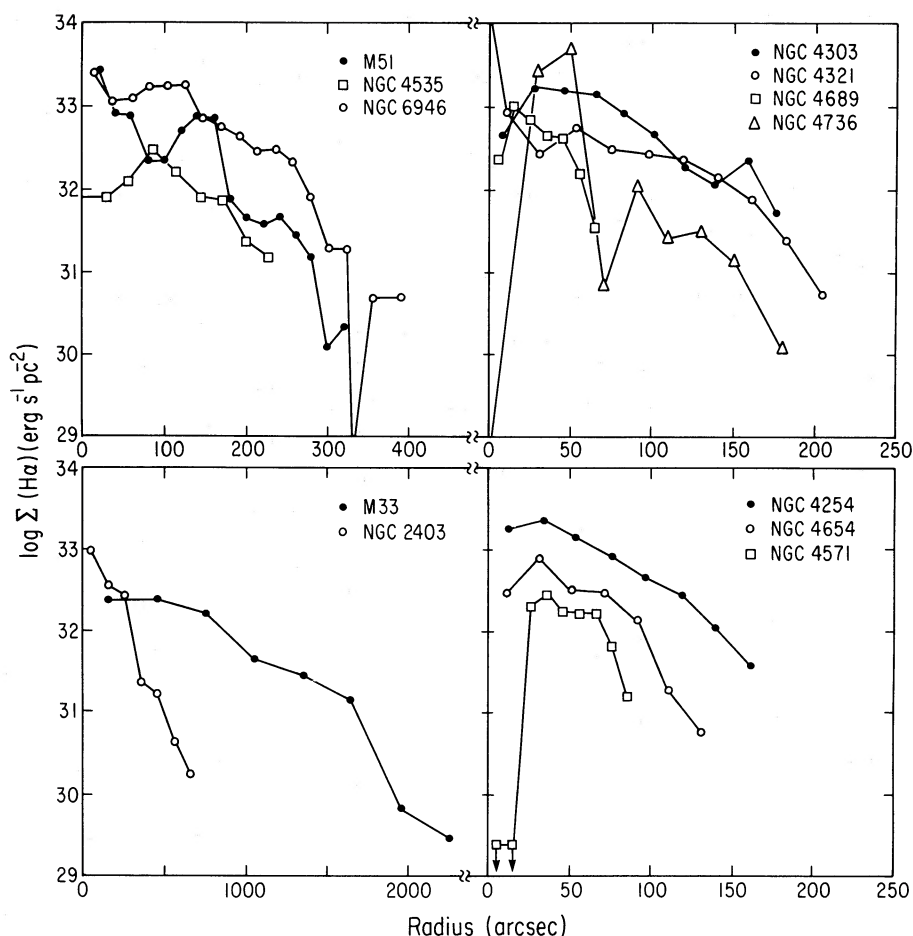
FIG. 2.—Radial distributions of Hα emission-line surface brightness

more sensitive to the galaxy sample, so it is important to use a common set of galaxies for all of the comparisons. We performed regressions on two samples, all 27 galaxies (Hubble types Sa–Sc), and the 19 Sc galaxies alone, in order to test whether the results are sensitive to the range of galaxy types under consideration. The results are summarized in Table 3.

Table 3 confirms most of the general conclusions drawn earlier. Hα emission is strongly correlated with H I and total gas density, but the correlation with H_2 density is barely significant. The correlations with H I and total density are weaker for the Sc subsample, which probably reflects the much smaller range in densities and SFRs within that group, but the correlation with H_2 is weak in both cases, indicating that the scatter is not mainly due to a change in the Hα versus H_2 relation with morphological type. The correlation between FIR emission and H_2 density is considerably stronger, as good as with H I;

this may be evidence for the extinction problem at Hα, but it also could well be due to a coupling between gas (and dust) density and FIR emission independent of the SFR. Also note that Hα and FIR emission are more strongly correlated with each other than with either H I or H_2 density. Overall there is no evidence here to suggest that CO emission is more strongly coupled to the global SFR than H I or the total gas density.

The relatively strong coupling between the SFR and H I surface density (relative to the molecular density inferred from CO measurements) observed here is opposite to the trend observed when the total masses of atomic and molecular hydrogen are correlated with the SFR. These contradictory results may be reconciled when one considers the spatial distribution of the H I. In most disk galaxies the bulk of the atomic gas lies at radii beyond the star-forming disk, and thus the total H I luminosity or mass may bear little relation to the conditions in the region where massive star formation is taking place. In Figure 3 we have compared the SFR with the H I density within the optical disk, so it may not be surprising that the correlation is much stronger. Kenney and Young (1988b) find a similar improvement in the SFR versus H I mass correlation when only the H I within the optical disk is considered.

Based on these results, we tentatively attribute part of the poor Hα–H_2 correlation to the effects of extinction at Hα, but most of it must be due to other causes. The most likely candidates in our view are a large variation in the conversion factor between CO intensity and H_2 column density, and/or a

TABLE 3

RANK CORRELATION COEFFICIENTS

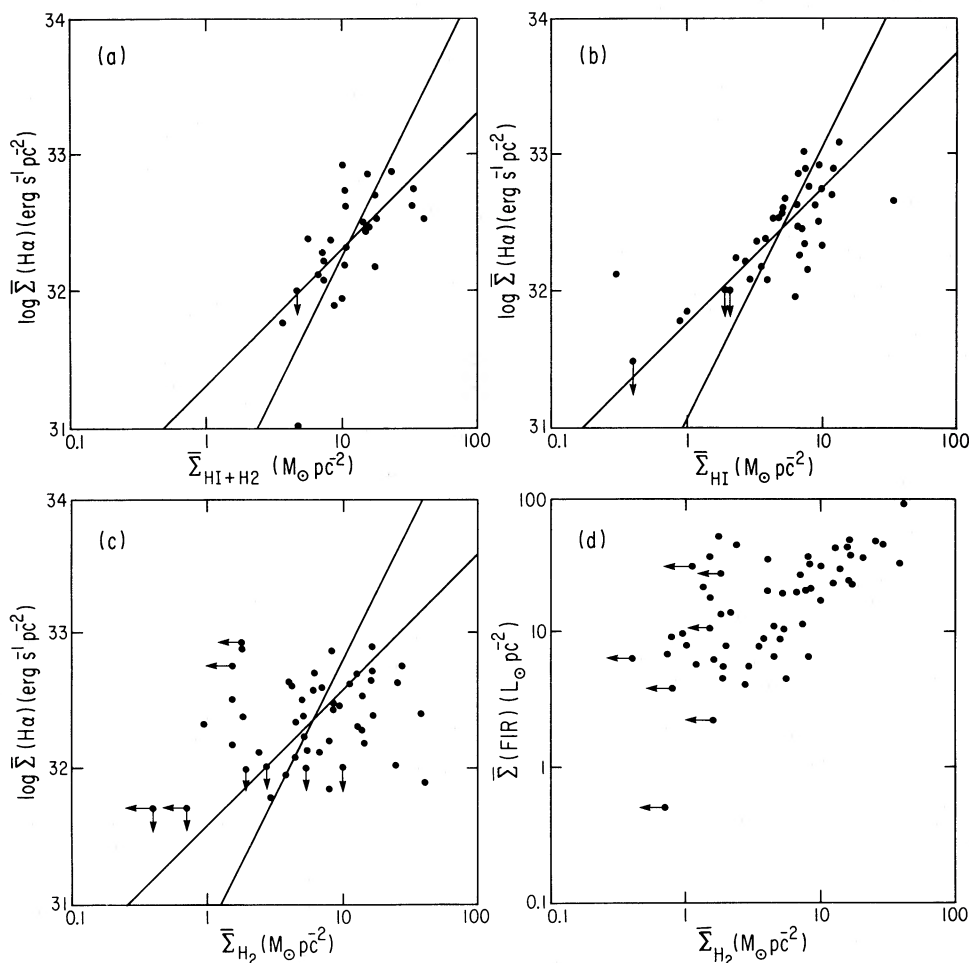| SURFACE DENSITY	ALL GALAXIES		Sc GALAXIES	
	$\Sigma(H\alpha)$	$\Sigma(FIR)$	$\Sigma(H\alpha)$	$\Sigma(FIR)$
H I	0.78	0.59	0.52	0.40
H_2	0.27	0.53	0.21	0.52
H I + H_2	0.70	0.79	0.49	0.76
Hα	...	0.79	...	0.76

Fig. 3.—Dependence of integrated Hα or far-infrared surface brightness, averaged over the disk, on the average surface density of gas for the galaxies listed in Table 2. The lines in each diagram denote the expected correlations for Schmidt laws with power law index $N = 1$ and 2. (a) Dependence of Hα surface brightness on the total gas surface density. (b) Dependence of Hα surface brightness on the mean H I surface density. (c) Dependence of Hα surface brightness on the mean H_2 surface density, as derived from the CO intensity. (d) Dependence of the far-infrared surface brightness on mean H_2 surface density.

genuine absence of coupling between the SFR for massive stars, averaged over an entire galaxy, and the mean molecular gas density. The latter could arise, for example, if the molecular gas component were coupled to a low-mass star formation mode, rather than the massive stellar population traced by Hα, or if the SFR were strictly governed by the volume density rather than the surface density of gas. Perhaps the most likely explanation for the scatter, however, is a large variation in the conversion factor between CO intensity and H_2 density among the galaxies in our sample, which could mask a much stronger underlying correlation between the SFR and actual H_2 density. The reader is referred elsewhere for discussions of this very controversial issue (Kenney 1987; Maloney 1987; Verter 1987). Whatever the explanation, the coupling between global star formation rate and CO emission appears to be considerably more complex than had been originally inferred.

Despite these uncertainties, the results above demonstrate that the average massive SFRs in galaxies, as traced by the Hα emission, can be loosely fitted by a power-law function of the total gas density, with a slope which is intermediate between the Schmidt's (1959) original value $n = 2$ and more recent claims of $n \approx 1$ based on CO studies. This provides some foundation for models of galactic evolution based on a single inte-

grated Schmidt star formation law, although the scatter of the observed relations is sufficiently large that one must question the physical significance of the correlation. Data covering a larger range of gas densities and galaxy types would be very useful for defining the range of conditions over which a global Schmidt law is useful.

b) Radial Distribution of Massive Star Formation

More direct information on the star formation law can be obtained if we examine the radial behavior of the gas and SFR distributions within individual galaxies. Figure 4 compares the radial profiles of Hα emission, red starlight (from Schweizer 1976), H I, and CO emission in NGC 4254, a representative Sc galaxy in our sample.

Over most of the star-forming disk in NGC 4254, the Hα distribution is well represented by an exponential profile, with a scale length which is similar to that of the stellar disk. The Hα profile shows a depression near the center of the galaxy, which may represent a real falloff in the star formation, or alternatively may be due to an increase in extinction near the galactic center. This general profile shape, with an outer exponential disk, sometimes accompanied by a central depression, is characteristic of most spiral galaxies (Hodge and Kennicutt 1983b).
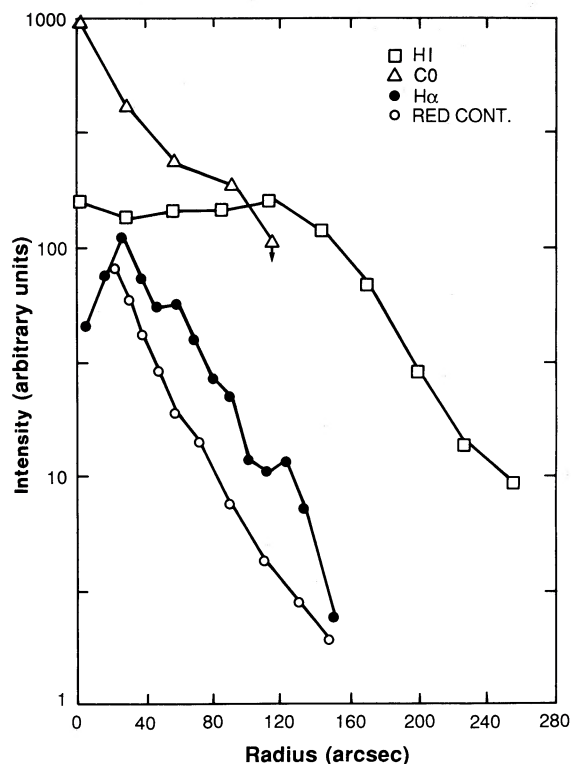
FIG. 4.—Radial profiles of H I, CO, Hα, and red continuum surface brightness in NGC 4254. Data are plotted on a relative scale, but the H I and CO profiles are normalized to a common surface density scale. The truncation of the Hα profile at a radius of 150″ is real.

In a small fraction of spirals, including the Galaxy and M31, the central depression is dominant, and the star formation is effectively concentrated in a ring (Hodge and Kennicutt (1983b).

Figure 5a compares the e-folding scale lengths of the H II region disks (exclusive of the central depressions, when present) with the corresponding scale lengths of the stellar disks, as measured from broad-band surface photometry in the literature. There is a strong correspondence between the radial distributions of young stars and the background stellar population, confirming earlier work by Hodge and Kennicutt (1983b) and Freedman (1984). In most spiral disks the integrated starlight is dominated by intermediate-age (1–5 Gyr) giants and young main-sequence stars of a few solar masses (e.g., Searle, Sargent, and Bagnuolo 1973; Kennicutt 1986), so our result implies that the large-scale star formation distribution in these systems has not changed radically over lifetime of the disk, or at least over the past few billion years. Furthermore, since the integrated starlight effectively traces the distribution of a much lower mass stellar component than the Hα emission, the correspondence in scale lengths offers some qualitative reassurance that the initial mass function does not change radically with galactic radius, at least for those galaxies whose Hα distributions are well represented by exponential disks.

Several authors have pointed out that the CO profiles of many galaxies also follow the Hα and stellar disks (Young and Scoville 1982a; Scoville and Young 1983; Solomon et al. 1983; DeGioia-Eastwood et al. 1984; Tacconi and Young 1986), and Figure 5b compares the Hα and CO scale lengths for the galaxies in our sample. A correlation is indeed apparent, but the scatter is much larger than in Figure 5a. In a few well-studied galaxies (e.g., NGC 6946, M51) the scale lengths of the CO, Hα, and stellar disks are nearly identical, while in others, especially early-type spirals or CO–weak galaxies such as M33 or NGC 2403, the CO and Hα distributions are essentially uncorrelated. An illustration of the latter is shown in Figure 6, which compares the distribution of Hα emission, blue light (Boroson 1981), H I, and CO emission in the Sb galaxy NGC 2841. The Hα emission shows the typical exponential decline with radius, but over a region where the gas density remains essentially constant; a Schmidt law clearly cannot describe the large-scale star formation in such galaxies.

In most of the galaxies in our sample there is little correlation between the radial distribution of H I and SFR. In general, the H I distribution falls off much more slowly with radius than any of the other gaseous or stellar components. In many spirals this can be explained by the predominance of molecular gas in the inner disk, but the H I tends to be more extended even in CO–weak galaxies. The similarity in radial distributions of Hα and CO emission (relative to the H I distribution) is in marked
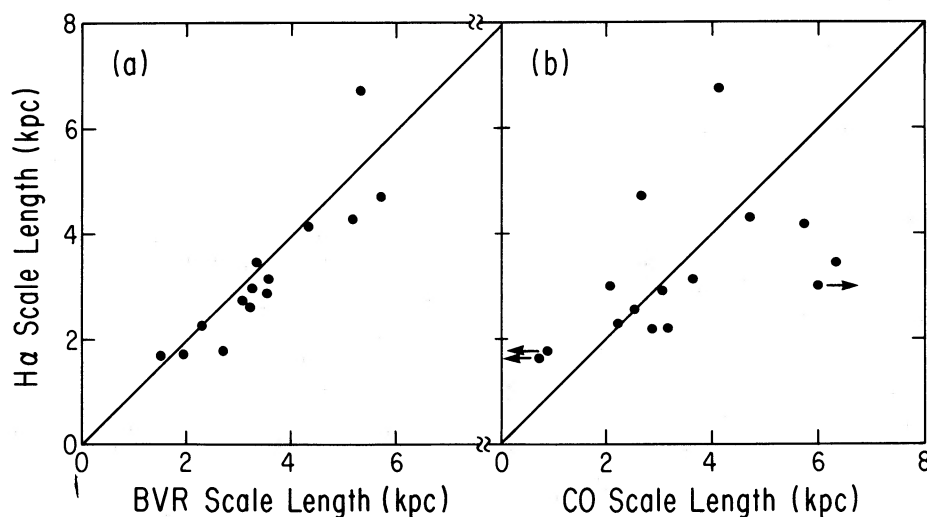

FIG. 5.—Comparison of the exponential scale lengths of the Hα disks with the corresponding scale lengths of the stellar disks (left) and the CO emission (right)
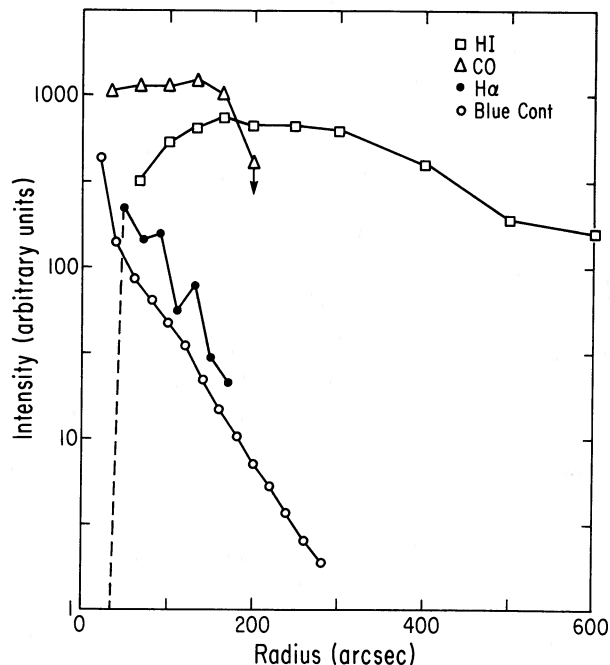
FIG. 6.—Radial profiles of H I, CO, Hα, and blue continuum surface brightness in NGC 2841. Notation is the same as in Fig. 4. Note that the absolute Hα surface brightness in NGC 2841 is much lower than in NGC 4254 (Fig. 4).

contrast to the results of Figure 3, which show the globally averaged density of star formation to be much more strongly coupled to the H I density. We can offer no explanation for this paradox, except to note that it is the total gas density, largely independent of phase, which appears to be most directly coupled to the massive SFR, as discussed later.

Any correlations between gas density and the SFR break down completely in the outer disk. In NGC 4254 and NGC 2841, for example, the H II region disks terminate at radii of 150″ and 170″, respectively, while the gas disks extend smoothly to much larger radii (see Figs. 4, 6). All of the galaxies in our sample possess star-forming disks which are confined well inside their gas disks (there may be similar cutoffs in the underlying stellar disks, as discussed in § VI). In some cases the star formation thresholds occur at approximately the radius where molecular gas begins to dominate over H I, but there are many exceptions, including galaxies where the star-forming disk is truncated well within the molecular-dominated disk (e.g., NGC 4569), and other cases where the threshold occurs well outside the main CO disk (e.g., M33, M101, NGC 2403). Similar star formation thresholds have been observed previously in irregular galaxies by Davies, Elliott, and Meaburn (1976), Hunter and Gallagher (1986), Skillman (1987), and Ohta, Sasaki, and Saito (1988), for spirals by Guiderdoni (1987), Nakano et al. (1987), and van der Hulst et al. (1987), and in the solar neighborhood by Kulkarni and Heiles (1987).

c) The Form of the Star Formation Law

Figure 7 shows the relationships between the azimuthally averaged Hα surface brightness and total (H I + H₂) gas surface density in NGC 4254 and NGC 2841. Each point shows the gas density and Hα brightness averaged at a given radius, with lines connecting points at adjacent radii. The number of points is limited by the spatial resolution of the CO data.

If gas density is the only parameter regulating the SFR, as is often assumed, then curves like those in Figure 8 would uniquely define the form of the star formation law. As shall be demonstrated later, however, other parameters influence the SFR, and the star formation law itself changes with radius within individual galaxies. Consequently, the relations in Figure 8 should be regarded only as describing the general features of the star formation law, and not its local form within the galaxies.

In NGC 4254 there is a large range in both the gas density and in the SFR per unit area, and the SFR–density relation shows three distinct regimes. At high gas densities, $\Sigma_H > 4 \ M_\odot$ pc^{-2}, the SFR increases smoothly with density; indeed, this part of the relation is well represented by a Schmidt power law (eq. [2]), with $N \approx 1.3$. Below a gas density of 4 $M_\odot$ pc^{-1}, however, the SFR drops abruptly. This is the threshold at the outer edge of the disk which was discussed earlier; at gas densities below 3–4 $M_\odot$ pc^{-2} there is no measured Hα emission. Between these two regimes is a transition region where the SFR increases very sharply with density, much more steeply than a standard Schmidt law. In NGC 4254 this transition is quite abrupt and is not well resolved by our data, but in some galaxies this transition region can extend over a few kiloparsecs (see Fig. 8).

The turnover in the star formation law near the threshold density can often be seen in previously published plots of SFRs versus density (e.g., Madore, van den Bergh, and Rogstad 1974). If one attempts to fit the entire SFR–density relation to a single power law, a relatively high value for the index will be derived. This effect may partially explain the anomalously high values of N which have often been reported in the literature.
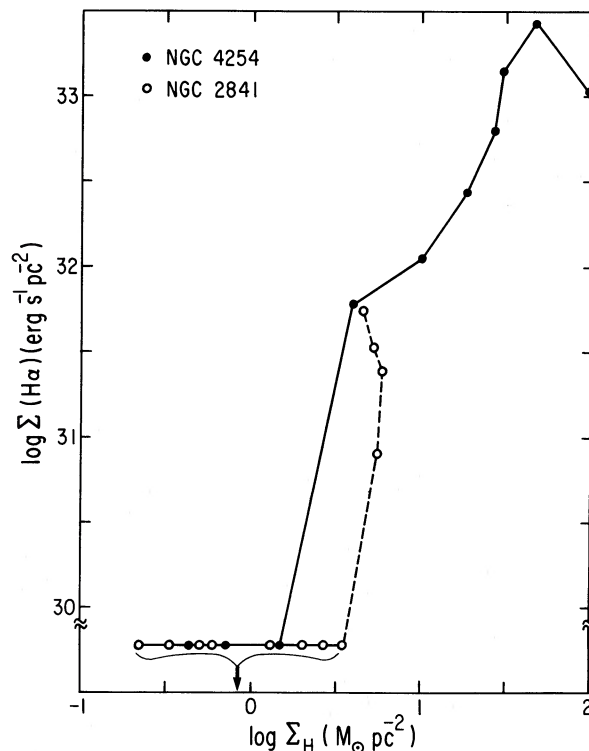

FIG. 7.—Dependence of Hα surface brightness on total (H I + H₂) hydrogen surface density for NGC 4254 and NGC 2841, as derived from the radial distributions in Figs. 4 and 6. The points at the bottom denote regions where no Hα emission was detected.
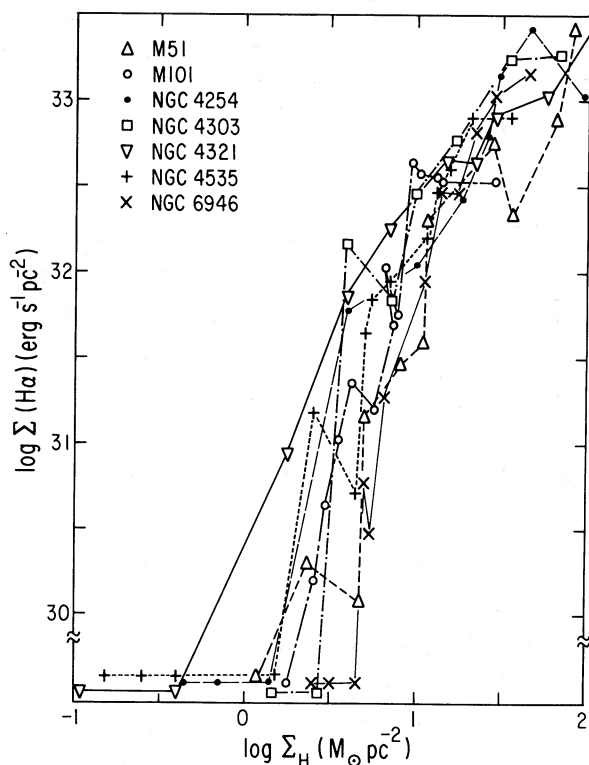
Fig. 8.—Dependence of Hα surface brightness on total (H ɪ + H₂) hydrogen surface density, for seven giant Sc galaxies. Each point represents the Hα and gas densities averaged at a given galactocentric radius, and lines connect points at adjacent radii. The points at the bottom denote regions where no Hα emission was detected.

NGC 2841 possesses lower gas densities and SFRs over most of its optical disk, and the character of its star formation law is somewhat different. The little star formation that does occur in NGC 2841 is not correlated with gas density in any simple way; in some regions the slope of the SFR–density relation is negative! At first glance the star formation laws in NGC 4254 and NGC 2841 appear to be completely different, but upon closer examination they share many similar features. Both galaxies possess star formation thresholds at a similar surface density, and below this value Hα emission is suppressed in both systems. The main difference appears to be that NGC 2841 lacks a high-density inner disk where the SFR is monotonically correlated with gas density. Instead, its main star-forming disk lies at low densities which correspond to the threshold region in NGC 4254, where the SFR increases steeply (and not necessarily monotonically) with gas density.

NGC 4254 and NGC 2841 were chosen as examples because they exhibit the extreme range of SFRs in our sample, and the other galaxies we studied show SFR–density relations which fall within this range of behaviors. For example, Figure 8 compares the radial SFR–density relations for the seven luminous Sc galaxies in our sample, including NGC 4254. There is a gratifying uniformity in these star formation laws, especially at high gas densities, where not only the slopes ($N = 1.3$–1.5), but even the zero points are similar. This is the best evidence to date for something approaching a universal star formation law, at least over this range of gas densities and galaxy types. Figure 8 also shows well-defined star formation thresholds in all of the galaxies, but the value of the threshold density clearly is not constant.

We have determined threshold surface densities for all of the galaxies in our sample, and a histogram of these densities is shown in Figure 9. In galaxies with well-measured Hα or H ɪɪ region profiles the threshold radius was defined to be the point where a strong break in the exponential profile occurs. In most cases this radius can be defined to an accuracy of ± 10%. In the few cases where this break could not be as easily defined, the threshold radius was defined to be the distance to the outermost detected H ɪɪ region. Figure 9 includes all of the galaxies in Table 1 with Hα data, as well as three late-type galaxies (NGC 628, 925, 2366) for which only Hα and H ɪ distributions are available, but which contain such extended H ɪɪ region disks that the contribution of molecular gas at the threshold radius should be negligible. The surface densities are expressed both in terms of hydrogen mass density $(M_\odot \text{ pc}^{-2})$, and an equivalent column density, in units of 10^{20} H atoms cm^{-2}.

The range of threshold densities in Figure 9, 1–$10\ M_\odot$ pc^{-2} or 10^{20}–10^{21} H cm^{-2}, is similar to the range reported by previous investigators. The dispersion in densities is real. In galaxies such as NGC 4736 and NGC 4569, for example, the star formation is suppressed at surface densities of 10–$40\ M_\odot$ pc^{-2}, nearly an order of magnitude higher than the corresponding threshold densities in M101 or M33; indeed, almost all of the star formation in the latter occurs at densities which are below the threshold value in NGC 4736 and NGC 4569. This large range in the observed star formation laws provides an important clue to the underlying physical mechanism which regulates the star formation.

IV. GRAVITATIONAL STABILITY AND STAR FORMATION THRESHOLDS

An abrupt decrease in star formation at low gas densities is expected from simple gravitational stability considerations. Below a critical density the gas disk is stable against the growth of large-scale density perturbations, and consequently one would expect cloud growth and star formation to be strongly suppressed. Guiderdoni (1987) has noted that the observed star formation threshold densities in spirals are of the same order as those expected from disk stability models. In this
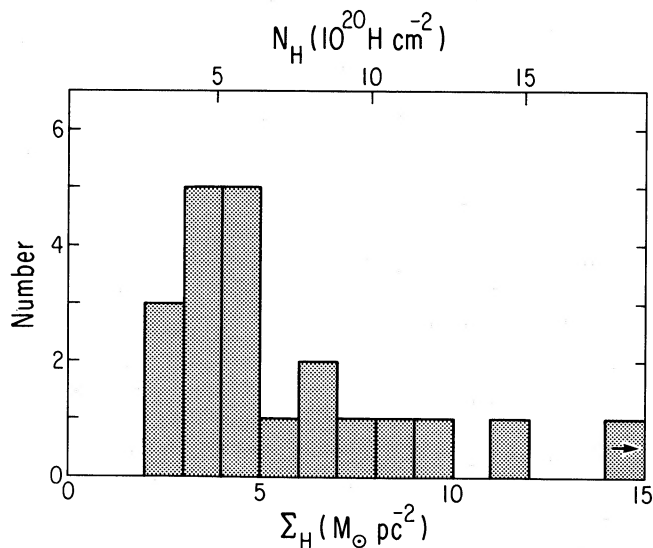

Fig. 9.—Distribution of threshold column densities in the sample. The bottom scale is in units of total (H ɪ + H₂) hydrogen mass surface density, and the top scale is in units of hydrogen column density.

section we derive the expected stability properties of the galaxies in our sample, and compare the results with the observed distributions of gas and star formation.

The stability condition for self-gravitating disks has been discussed by several workers (Toomre 1964; Goldreich and Lynden-Bell 1965; Elmegreen 1979; Cowie 1981; Jog and Solomon 1984a, b; Larson 1983, 1988). In the simplest case of a thin isothermal gas disk, instability is expected if the surface density exceeds a critical value (Toomre 1964; Cowie 1981):

$$\Sigma_c = \alpha \frac{\kappa c}{3.36 G}, \qquad (4)$$

where c is the velocity dispersion of the gas, κ is the epicyclic frequency, and α is a dimensionless constant near unity. Equation (4) strictly applies only to thin stellar disks ($\alpha = 1$), but the same condition, with $\alpha = 1$, will describe the stability of a thin gaseous disk embedded in a more massive stellar disk (e.g., Cowie 1981). In general, one expects $\alpha < 1$ in a realistic gas/stellar disk, due to the onset of two fluid instabilities (Jog and Solomon 1984a, b). We shall refer to the density in equation (4) as the "critical density."

The radial dependence of the critical density in a particular galaxy can be derived if its rotation curve and the gas velocity dispersion are known. Velocity dispersions have been measured for the H I and CO disks in our own Galaxy (e.g., Burton 1971; Lizst and Burton 1983; Stark 1984; Clemens 1985), and for the H I in a few external galaxies (van der Kruit and Shostak 1984; Murray and Dickey, private communication). The measured values lie in the range $c = 3$–10 km s^{-1}. The same data indicate that c is approximately constant within individual disks. This is a very useful result, because it means that the radial dependence of the critical density can be estimated directly from the rotation curve of a galaxy.

We have used equation (4) to derive the critical density as a function of radius for each of the galaxies in Table 1. The epicyclic frequency

$$\kappa = 1.41 \frac{V}{R} \left(1 + \frac{R}{V} \frac{dV}{dR} \right)^{1/2} \qquad (5)$$

was derived directly from the rotation curve. In order to keep the model as simple as possible, we have assumed a constant gas velocity dispersion $c = 6$ km s^{-1} in all of the galaxies, and a constant value for the stability constant α. We shall then use the observations to derive the best fitting average value for α. This is almost certainly oversimplistic, but we wish to test how well a simple gravitational stability model can reproduce the observed star formation thresholds, with a minimum of assumptions and free parameters. Note that the derived value for the stability index scales inversely with the assumed value for the velocity dispersion.

Under these simplifying assumptions the radial dependence of the critical density in a disk is determined completely by its rotation curve. For a flat rotation curve and $c = 6$ km s^{-1}, the stability condition takes a very simple form:

$$\Sigma_c \, (M_\odot \text{ pc}^{-2}) = 0.59 \alpha V \text{ (km s}^{-1})/R \text{ (kpc)}. \qquad (6)$$

In order to illustrate the behavior of the critical density in a typical late-type galaxy, Figure 10 shows the radial dependence of the observed gas surface density Σ_g (total H density multiplied by 1.45 to include other elements), the critical density Σ_c (assuming $\alpha = 1$ for the moment), and the ratio Σ_g/Σ_c for NGC 6946, a nearby Sc galaxy which has been extensively studied in
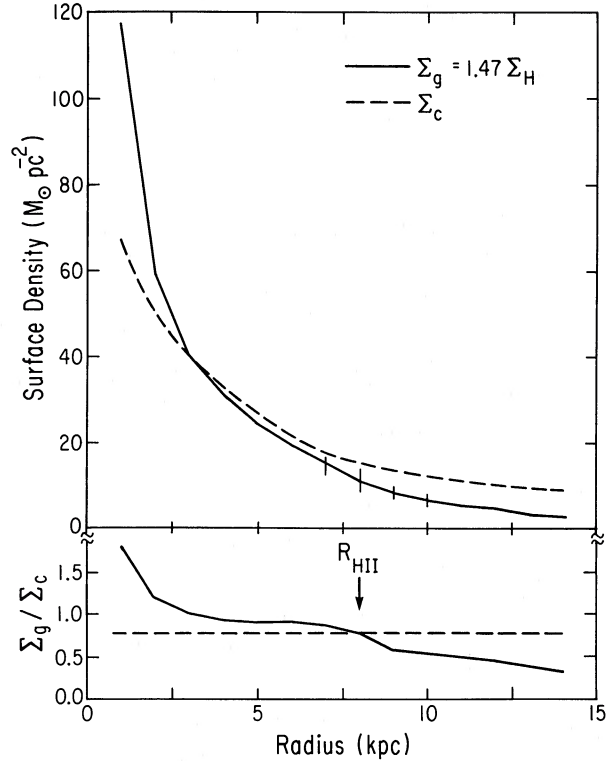

FIG. 10.—Top panel shows the radial distribution of total (atomic and molecular) gas surface density in NGC 6946 (solid line), and the radial dependence of the threshold surface density for gravitational stability, from eq. (4). Bottom panel shows the radial dependence of the ratio of these two densities. The vertical arrow denotes the radius of the H II region disk, and the horizontal dashed line indicates the value of Σ_g/Σ_c at this radius.

CO, H I, and Hα (Young and Scoville 1982a; Tacconi and Young 1986; Bonnarel, Boulesteix, and Marcelin 1986). The radial behavior of the critical density is remarkably similar to the actual gas distribution in NGC 6946; the ratio Σ_g/Σ_c remains constant to within a factor of 4–5 over a hundredfold range of gas density. The gas density decreases slightly faster with radius than the critical density, with the ratio reaching a value of ~ 0.7 at the outer radius of the H II region disk (indicated by the arrow in Fig. 10). Hence the star formation in NGC 6946 is restricted to regions where $\Sigma_g/\Sigma_c > 0.7$ and is suppressed in regions where the ratio falls below this value. The general properties of the star formation in NGC 6946 could be explained by gravitational stability if the stability parameter $\alpha = 0.7$.

These general results are shared by all of the active star-forming galaxies in our sample. Figure 11 shows the radial dependence of the ratio Σ_g/Σ_c for 12 Sc galaxies (M33, M51, M101, NGC 2403, 4254, 4303, 4321, 4535, 4647, 4654, 4689, 4946). The Sab–Sb galaxies NGC 4569, 4736, and 7331 are also plotted, because they also exhibit very active inner star-forming disks, and the unusually high threshold densities in NGC 4569 and NGC 4736 provide a good test of the stability model. In this diagram the radial coordinate is normalized to the outer radius of the H II region disk, i.e., the observed threshold radius. Hence active star formation in these galaxies occurs in the region to the left of the vertical line in Figure 11.

Figure 11 demonstrates that within the star-forming disks of these galaxies, the ratio of gas surface density to the critical density for stability usually does not change by more than a
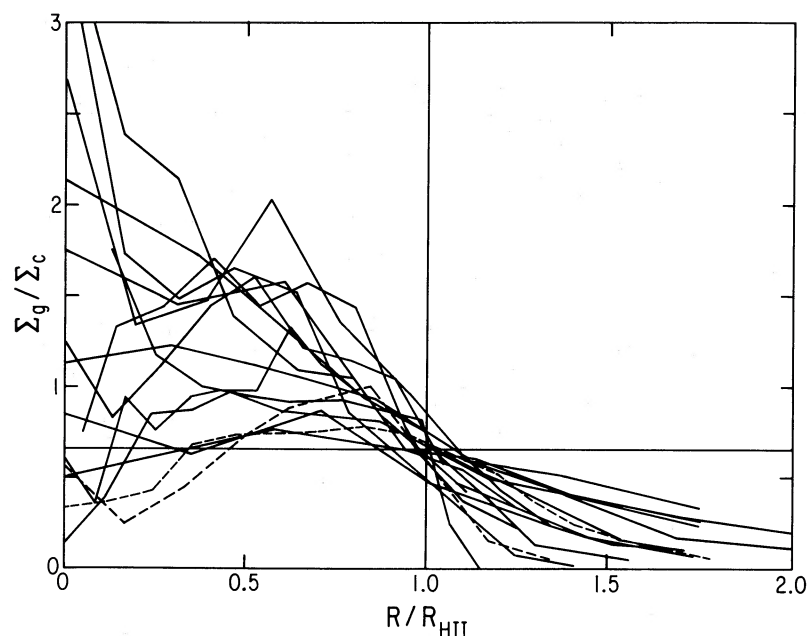
FIG. 11.—Radial dependence of the ratio of gas surface density to the critical density for gravitational stability (eq. [4]), for the galaxies with active star-forming disks. The radial coordinate is normalized to the radius of the H II region disk. The horizontal line indicates the value for the stability parameter ($\alpha = 0.67$) which best fits the observed star formation thresholds. Dashed lines denote M33 and NGC 2403.

factor of 2–3. This tendency for the gas disks to lie near the gravitational stability limit was first noted by Quirk (1972), using H I data which were available at that time, and our results confirm that this is a general property of the gas disks in late-type galaxies. There are two galaxies, M33 and NGC 2403 (indicated by dashed lines), in which the observed gas density lies below the threshold within much of the inner star-forming disk. These are both lower luminosity galaxies with unusually weak, small CO disks, and the deviation of these objects from the general trend observed in more luminous galaxies may indicate a breakdown of the stability model, or it may be caused by a difference in the CO–H_2 conversion.

Figure 11 also shows that there is a critical value for the stability parameter, indicated by the horizontal line at $\alpha = 0.67$, which defines the outer edge of the active star-forming region in all of the galaxies. The agreement between the locations of the thresholds predicted by the simple stability model and the observed thresholds is quite striking; the values of $\alpha = \Sigma_g/\Sigma_c$ at the threshold radius all lie within the range 0.5–0.85, even though the absolute values of the threshold density in the galaxies vary by more than a factor of 10 (see Fig. 9).

Figure 12 illustrates how well the simple stability model reproduces the observed star formation thresholds in these
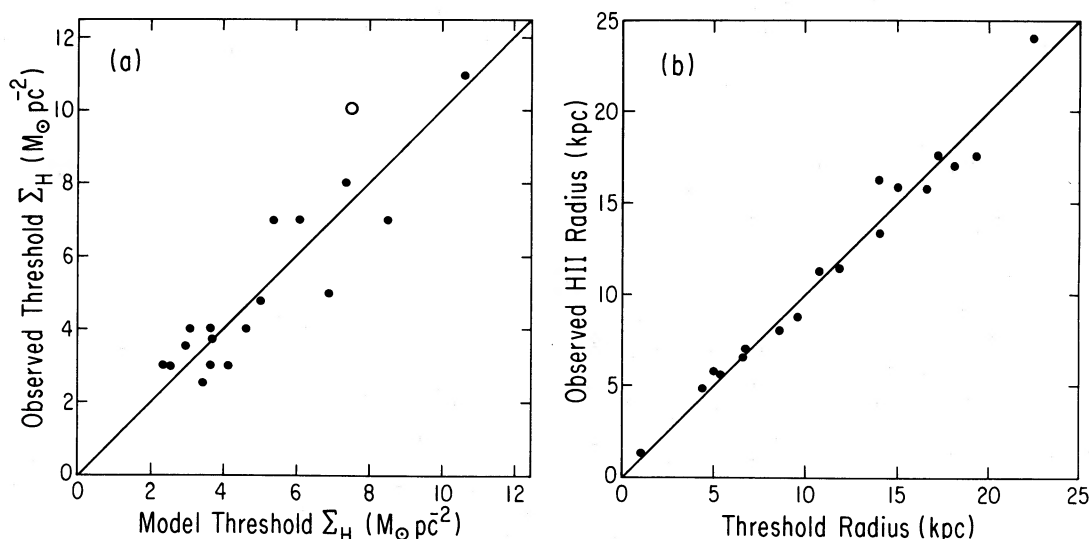

FIG. 12.—(a) Comparison of the observed star formation threshold densities for the galaxies in Fig. 11 with the values at which the gas density drops below the critical density for gravitational stability, as given by eq. (4) with $\alpha = 0.67$. (b) Comparison of the observed radii of the H II region disks with the radii where the gas surface density drops below the critical density for gravitational stability.

galaxies. For each spiral in Figure 11 (plus NGC 628, 925, 2366) we computed the radial dependence of the critical density Σ_c, using equation (4) with $c = 6$ km s^{-1} and the mean value $\alpha = 0.67$ derived above. We then compared this to the radial dependence of the actual gas, surface density in each galaxy and determined the radius and surface density where the gas density dropped below the predicted threshold value. Figure 12a compares the predicted threshold gas densities with the actual observed densities at the outer edge of the star-forming disks, while Figure 12b compares the predicted threshold radii with observed radii of the H II region disks. Since we used the observed thresholds to derive the average value of α, we have forced the predicted and observed values to agree on average, but what is remarkable in Figure 12 is the small scatter, especially given the simple assumptions built into our stability model. This low scatter ($\pm 18\%$ in density and $\pm 8\%$ in radius) may be partly fortuitous, but in any case it is clear that a simple gravitational stability model can reproduce the observed radial extents of the global star formation and the qualitative behavior of the gas distributions in actively star forming galaxies.

We can now understand the large range in threshold densities observed in our sample (Fig. 9). The galaxies with unusually high thresholds, such as NGC 4569 and NGC 4736, are characterized by very rapid rotation in their inner disks, and consequently the critical densities for gravitational stability are very high. Even though these galaxies possess dense inner gas disks, the density gradient is steeper than the corresponding $1/R$ falloff in the critical density, and the star formation is suppressed at relatively high densities and small radii. On the other hand, the galaxies with very low thresholds are characterized by lower rotation velocities and rotation curves which rise more slowly with radius, and consequently in those systems the critical density at a given radius is considerably lower. The rotation properties of the late-type galaxies, combined with their extended gas disks, allow active star formation to persist to relatively low densities and large radii.

The results in Figures 11–12 apply to galaxies with active star formation taking place throughout their inner disks, where the azimuthally averaged gas and Hα profiles are representative of the general conditions in the disks. Earlier type galaxies, which are generally characterized by lower levels of star-

forming activity (e.g., NGC 2841), show a somewhat different behavior. This is illustrated in Figure 13, which shows the radial distributions of Σ_g/Σ_c in nine Sab–Sb galaxies (NGC 2841, 4192, 4216, 4394, 4548, 4579, 4388, 4639, 4698) and one red "anemic" galaxy, NGC 4571, which is classified as an Sc galaxy, but has a SFR which is more typical of Sa–Sb galaxies. Hα distributions are only available for three galaxies (NGC 2841, 4548, 4571), so we have normalized the radial coordinate in Figure 13 to the isophotal radius $D(0)/2$ from de Vaucouleurs, de Vaucouleurs, and Corwin (1976). It is important to emphasize that the gas density in many of these galaxies often varies by large amounts at a given radius, the averaged radial profiles are not as meaningful as in Figure 11.

The stability properties of the gas in these galaxies are qualitatively different from the active star-forming galaxies shown in Figure 11. If we assume that the same velocity dispersion and stability index ($\alpha \sim 0.7$) apply to these galaxies, then most are characterized by gas disks which are gravitationally stable, at least in terms of the azimuthally averaged density. Consequently we would not expect to observe active global star formation in these systems, and this is generally the case. On the other hand, the average densities in most of the disks is often sufficiently close to the threshold value ($0.2 < \Sigma_g/\Sigma_c < 0.7$) that one might expect star formation to take place in localized regions with modest density enhancements, such as spiral arms. This is indeed observed in some of the galaxies; for example, in NGC 4548, which is indicated by the dashed line in Figure 13, most of the H II regions are concentrated in a tight pair of spiral arms, at a radius corresponding to the peak in Figure 13. More complete CO and Hα data on these galaxies are needed, however, before we can test this hypothesis further.

In summary, our analysis of the stability properties of the disks has led to two significant results. First, the abrupt star formation thresholds that are observed in our sample can be identified with large-scale gravitational instabilities in the disk. A simple stability model can quantitatively reproduce the observed locations and densities of the star formation thresholds. Second, the radial distributions of gas in active star-forming galaxies closely follow the corresponding radial behavior of the threshold density for gravitational stability. Taken together, these results imply that the gas everywhere in the disk lies near the threshold for star formation. It is also
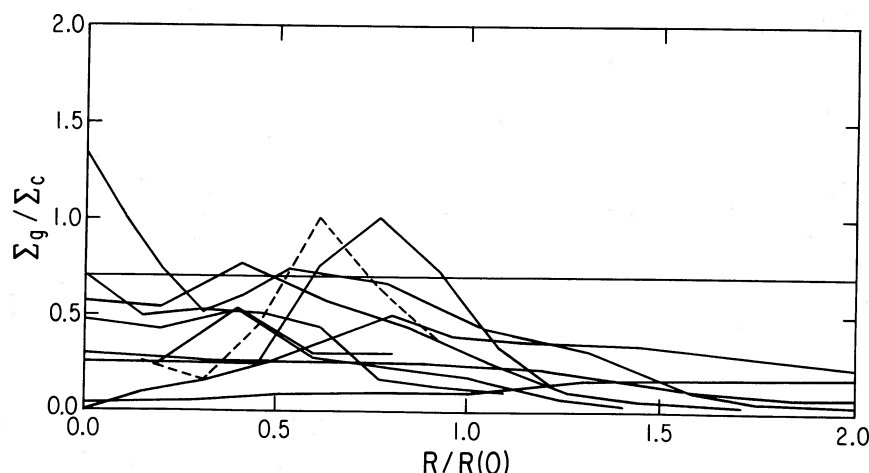

FIG. 13.—Radial behavior of the ratio of total gas surface density to the critical density for gravitational stability (eq. [4]), for early-type (Sab–Sbc) galaxies. The radial coordinate is normalized to the isophotal radius of the disk. The horizontal line indicates the value $\alpha = 0.67$ which best fits the observed star formation thresholds in late type galaxies. The dashed line denotes NGC 4548.

possible that the distribution of the gas itself may be determined in large part by the stability condition. The idea that large-scale Jeans instabilities are an important mechanism regulating the star formation and gas distributions was discussed in detail by Quirk (1972) and has been considered more recently in general terms by Fall and Efstathiou (1980), Larson (1983, 1988), and Guiderdoni (1987). A similar density threshold is predicted by the Oort model of Struck-Marcell and Scalo (1987). Our results provide quantitative confirmation of the basic aspects of this picture.

V. DISCUSSION: THE FORM AND PHYSICAL NATURE OF THE STAR FORMATION LAW

The standard Schmidt star formation model used in most galactic evolution models assumes a smooth, continuous power-law relationship between the SFR and the gas density. Our results introduce fundamental modifications in this picture. First, we find that the SFR is regulated by at least two parameters, the local gas density, and the ratio of this density to a local gravitational threshold density which is governed by the dynamical properties of the disk. (Other parameters may also regulate the SFR, as discussed later.) Second, the SFR–density law is not smooth and continuous, but rather changes abruptly from a steep nonlinear relation below the threshold density to a relatively shallow power law above the threshold. Third, since the critical density for stability is a strong function of galactocentric radius, the form of the star formation law itself must also change with radius within galaxies. For the same reasons, the systematic differences in the kinematic properties of galaxies as a function of Hubble type and luminosity should introduce corresponding differences in their star formation laws. Although this revised picture is clearly more complex than a simple Schmidt law, the basic form of the star formation law at a given location in galaxy can be readily predicted if the kinematic properties of the disk are known. Consequently, these results offer us not only a more accurate empirical description of the star formation law but also a physical basis for understanding its basic form.

Figure 14 illustrates in schematic form the behavior of the star formation law at four radii in a typical galactic disk. At any radius the star formation law can be divided into three distinct regimes, with the transitions between these regimes occurring near the critical density for gravitational stability. Since the critical density increases with decreasing radius (roughly as $1/R$ for a flat rotation curve), the curves in Figure 14 will shift to progressively higher densities as one proceeds from the outer part of the disk inward. Gas which is easily dense enough to form stars in the outer disk may lie unperturbed in the inner regions. Moreover, since the SFR above the threshold increases rapidly with density, the magnitude of the nonlinear jump in the SFR as gas crosses the threshold will be much higher at higher threshold densities.

For regions where the gas density exceeds the critical density (assuming $\alpha = 0.67$ in eq. [4]), the gas will be unstable to spontaneous gravitational collapse and star formation. For typical disk densities the time scales for growth of these perturbations are of order a few times 10^7 yr, with corresponding Jeans lengths and masses of order 1 kpc and $10^7 M_\odot$ for typical disk densities (Larson 1988). In this regime the average SFR is well approximated by a Schmidt-type power law, with index $N = 1.3 \pm 0.3$. This slope is significantly shallower than the values near $N = 2$ derived in the early H I studies, but it appears to be steeper than the linear density dependence indi-
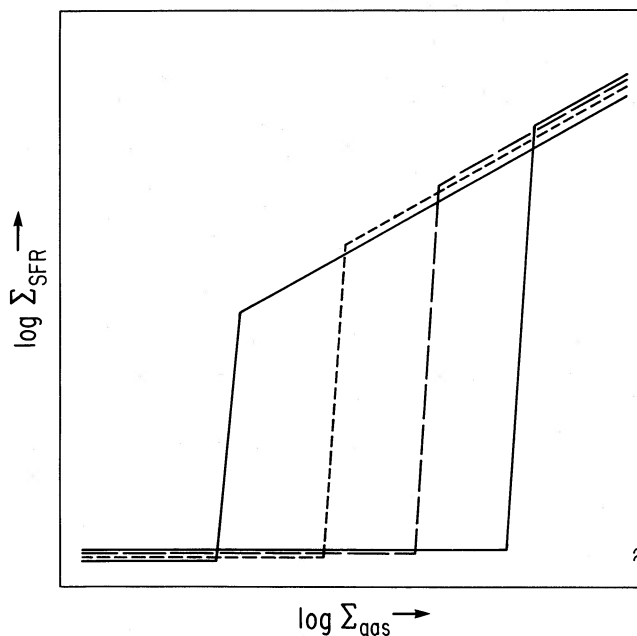

FIG. 14.—Schematic representation of the star formation law at 4 different radii in a galaxy. The curves to the right correspond to successively smaller radii and higher threshold densities.

cated by early CO studies. The index measured here should be treated with caution, however, because our SFR–density relations were derived from radial profiles, and gradients in extinction in the galaxies would tend to lower the derived slope of the best fitting power law. It is also possible that the SFR is influenced by some other parameter which varies systematically with radius, such as the stellar surface density of the disk, and this too could alter the apparent slope of the SFR versus gas density relation. Point-by-point observations of SFRs and gas densities are better suited for measuring the slope of the star formation law above the threshold, and an analysis of such data will be published in a future paper.

A detailed discussion of the physical nature of the star formation law in this high-density regime is beyond the scope of this paper. Larson (1987, 1988) has used several qualitative arguments to justify a Schmidt law with index $n = 2$. Talbot and Arnett (1975), Franco and Cox (1983), Ikeuchi, Habe, and Tanaka (1984), Dopita (1985, 1988), and Silk (1987) have developed more quantitative models of the star formation law in the high–SFR regime, under the assumption that the star formation is a self-regulating process on large scales. The self-regulating models predict a SFR which depends on both the gas surface density and the mass surface density of the disk, with effective Schmidt law indices in the range $N = 1$–2, which is at least qualitatively consistent with our observations. We defer a more detailed discussion of these models to a future paper.

Below the threshold density the gas disk is gravitationally stable, and the SFR drops sharply. In terms of the Toomre (1964) stability criterion in equation (4), we observe a star formation threshold corresponding to a stability criterion:

$$\alpha = 4.0/c \ (\text{km s}^{-1}) , \qquad (7)$$

where c is the velocity dispersion of the gas disk (the possibility of feedback between the SFR and the stability criterion itself will be discussed later). In regions where the gas density is well

below the critical density ($\Sigma_g/\Sigma_c \ll \alpha$), we would expect virtually no star formation to take place, and this is in accord with our observations. On the other hand, in regions where the density is only slightly below the critical value, local compression of the gas, for example from spiral arms or supernova shocks, may induce local instabilities and star formation. We suspect that this process is responsible for most of the star formation in the intermediate-type spirals, especially "grand-design" spirals such as M81, which exhibit active star formation in spiral arms, but virtually no star formation elsewhere. In many galaxies most or all of the disk may lie in this transition regime, where the gas density hovers just below the stability limit, as discussed in more detail in § VIa.

Our observations show that the SFR is a very steep function of density in the region near the threshold value, and this effect may account for the highly nonlinear star formation behavior observed in many galaxies, such as interacting galaxies or spirals with strong concentrations of star formation in their arms. The turnover in the slope of the star formation law near the threshold density provides a mechanism for producing both a highly nonlinear response of the SFR to gas density in regimes where the gas lies near or just below the threshold, as well as a relatively linear response in other, more gas-rich regions. We shall apply this result to the problems of star formation in spiral arms and starburst galaxies in the next section.

Finally, in regions where the average surface density of gas is much lower than the threshold density ($\Sigma_g/\Sigma_c \ll 0.2$), the disk will be stable against local density perturbations, and star formation will be completely suppressed. There are two types of environments where this regime will be important, regions of low gas density, such as the disks of S0–Sa galaxies or the outer disks of late-type spirals, or alternatively regions where the threshold density is very high, such as the near-nuclear regions of galaxies with high central mass concentrations. We discuss the possible implications of the threshold model for the latter environment in § VIf.

One might naively presume that the behavior of the star formation law near the stability limit is only relevant in a few regions, for example near the outer edge of the active star-forming disk. This misconception may explain why the thresholds have largely been ignored in the past, despite considerable observational evidence for their importance (e.g., Quirk 1972). Figures 11 and 13 demonstrate, however, that the gas disks in almost all spiral galaxies are almost always within a factor 2–4 above or below the threshold density, at virtually all radii. Consequently, the strong deviations from the Schmidt law which occur near the threshold are crucial for understanding the large-scale star formation throughout galactic disks.

VI. IMPLICATIONS AND POSSIBLE APPLICATIONS

In this section we discuss several possible applications of our results, including a number of observations which have been difficult to reconcile with a simple Schmidt star formation law. We conclude by summarizing those observations which are difficult to reconcile with the present results, and mention areas where new observations would be most useful.

a) Distributions of Gas and the Evolution of Galactic Disks

The radial distributions of gas in most of the galaxies we studied appear to follow closely the radial falloff in the gravitational threshold density, and it seems unlikely that this is merely a coincidence. Instead, this result suggests that gravita-

tional stability regulates both the SFR and the gas distributions themselves, as originally hypothesized by Quirk (1972). It is easy to visualize how this might occur. An initially gas-rich disk will experience active star formation until the surface density approached the critical value, then at that point the SFR (and thus the gas consumption rate) would rapidly decrease. This process would tend to leave the disk at or slightly below the critical density at all radii.

There are some problems with this picture, however. Observations of late-type spiral galaxies show that most have formed stars at approximately a constant rate over their lifetimes (e.g., Searle, Sargent, and Bagnuolo 1973; Tinsley and Danly 1980; Kennicutt 1983, 1986), but if the gas disks currently lie very close to the stability limit, we would expect star formation (and subsequent gas consumption) to drive the gas density below the threshold during the next few billion years, after which the SFR will be strongly curtailed. It seems unlikely that we would now observe most late-type galaxies at the same unique stage in their evolution. This paradox is similar to the well-known gas consumption problem for disk galaxies (e.g., Larson, Tinsley, and Caldwell 1980; Kennicutt 1983), but is even more severe, because the time scale for depleting the gas below the stability limit is considerably shorter than the time scale for completely exhausting the gas supply. This paradox was pointed out by Quirk and Tinsley (1973), who used it to argue that gas infall must be occurring to maintain the disk surface density above the threshold. The infall rates required by this hypothesis are uncomfortably large, several $M_\odot$ yr^{-1} for luminous Sc galaxies (Kennicutt 1983), although additional replenishment of the gas from stellar mass loss can alleviate part of the problem.

Another possibility is that the simplifying assumptions in our threshold model break down when describing the long-term evolution of the disks. For example, the assumption of a constant velocity dispersion for the gas disk is based on observations of actively star-forming galaxies, but it is possible that after the SFR is suppressed in a galaxy, the scale height and velocity dispersion of the gas disk gradually decrease, until global gravitational instability once again takes place. A similar feedback between the SFR and the gravitational stability condition could arise if the SFR is governed more directly by the volume density of gas, rather than the surface density. It should be straightforward to model the evolutionary behavior of a disk under such assumptions (e.g., Talbot and Arnett 1975), but it may be more difficult to obtain the spatially resolved observations of gas densities, kinematics, and SFRs which would be necessary to test these conjectures unambiguously.

b) Distributions of Molecular and Atomic Gas in Galaxies

It is tempting to hypothesize that the same gravitational stability mechanism might also be responsible for the relatively sharp radial transition between a molecular-dominated and H I–dominated interstellar medium in many galaxies. Elmegreen (1979), Cowie (1981), and Ikeuchi, Habe, and Tanaka (1984) have shown that gravitational stability considerations can account for the molecular ring in our own Galaxy (see § VIc). In order to test crudely this hypothesis for the galaxies in our sample, we measured the radius in each galaxy at which the surface densities of atomic and molecular gas are equal, and then examined the dispersion in total gas surface densities Σ_g, the critical densities Σ_c, and the ratios Σ_g/Σ_c at these "molecular threshold" radii. Since the transition from a
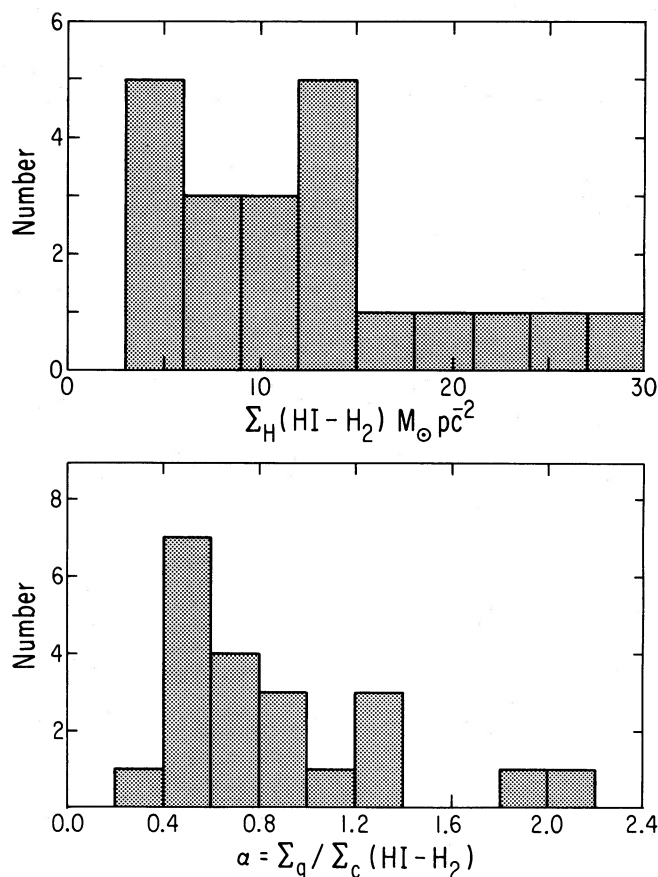
FIG. 15.—Top panel shows the distribution of "molecular threshold" densities, where the gas is half atomic and half molecular. Bottom panel shows the corresponding ratios of total gas density to the critical density for gravitational stability (eq. [4]).

molecular to atomic-dominated medium is quite abrupt in most galaxies, our results are not very sensitive to the precise definition of this radius.

If the growth of molecular clouds is governed by the same stability criteria which appear to regulate the SFR, we would expect to observe a relatively small dispersion in the values of Σ_g/Σ_c, comparable to what was found for the star formation thresholds. Figure 15 shows a histogram of this ratio, as well as a histogram of the total surface densities at the molecular threshold. A comparison of Figure 15a with Figure 9 shows that the molecular gas becomes dominant at surface densities which are several times higher on average than where the star formation thresholds occur, but the dispersion in "threshold" densities is similar in the two cases. On the other hand, the values of Σ_g/Σ_c show a dispersion of roughly an order of magnitude (Fig. 15b), nearly as large as the dispersion in absolute molecular threshold densities, and compared with less than a twofold range in Σ_g/Σ_c at the star formation thresholds (see Fig. 11).

Consequently, it appears, perhaps not surprisingly, that the gravitational stability of the disk is not the only important parameter which regulates the large-scale equilibrium between molecular and atomic gas in these galaxies. Although the stability model can reproduce some of the qualitative properties of the molecular and atomic gas distributions, other models based on very different mechanisms, such as the rate of passage through spiral arms (Wyse 1986) and dissociation of molecular

gas by young stars (Shaya and Federman 1987), seem to work at least as well. Other parameters, such as metallicity and dust content, may also be important.

This result also reinforces the earlier suggestion in our data that the onset of global active star formation is predominantly regulated by the self-gravity of the gas, independent of whether the gas is predominantly atomic or molecular. We find it somewhat surprising that the coupling between the SFR and molecular density is not stronger, since molecular clouds are thought to be the direct precursors to massive star formation. Perhaps the coupling between molecular gas and the SFR is a strictly local process, which is obliterated when we study the SFR on very large scales, or perhaps variations in the CO/H_2 ratio are introducing a spurious dispersion into Figure 15.

c) Distribution of Massive Star Formation in the Galaxy

The relationship between the SFR and gas density in our Galaxy has been discussed by several workers (e.g., Guibert, Lequeux, and Viallefond 1978; Güsten and Mezger 1983; Scoville and Good 1986). The SFR–density relation has usually been analyzed in terms of the Schmidt law, and indices in the range $N = 1.3$–2 have been derived. Here we examine whether the observations are consistent with the threshold model. Other studies of the gravitational stability of the Galactic disk have been carried out by Elmegreen (1979), Cowie (1981), and Ikeuchi, Habe, and Tanaka (1984).

The radial distribution of interstellar hydrogen in the Galaxy is shown in Figure 16 (top panel). The profile includes both atomic and molecular gas, taken from Sanders, Solomon, and Scoville (1984), using the $CO–H_2$ conversion in equation (3), and converted to a Galactic center distance of 8.5 kpc. Also shown is the distribution of giant H II regions (per square kiloparsec), taken from Scoville and Good (1986).
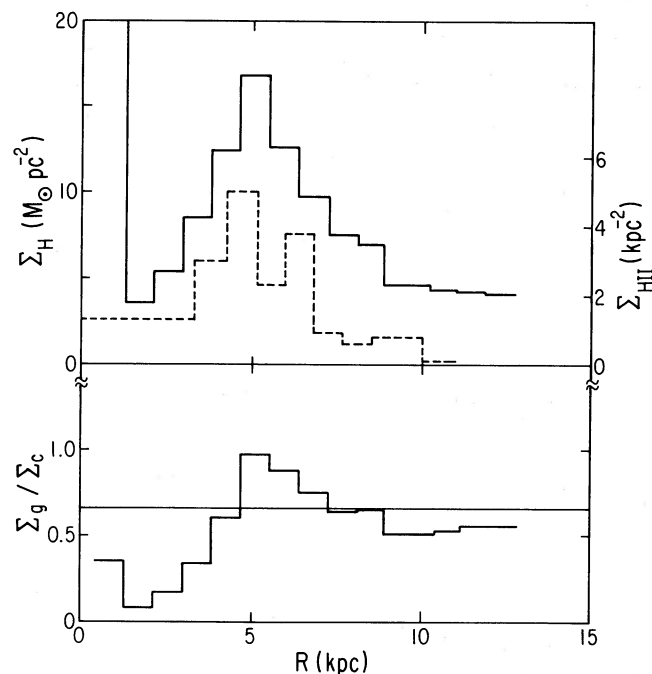

FIG. 16.—Top panel shows the radial distribution of total (H I + H_2) hydrogen surface density in the disk of the Milky Way Galaxy (solid line), and the surface density of giant H II regions (dashed line). Bottom panel shows the radial behavior of the ratio of gas density to the critical density for gravitational stability, as in Figs. 11 and 13.

We have used the rotation curve of Clemens (1985) and equation (4) to derive the radial dependence of the critical density in the Galactic disk, under the same assumptions that were applied earlier to the external galaxies. The bottom panel in Figure 16 shows the radial dependence of Σ_g/Σ_c, with the horizontal line indicating $\alpha = 0.67$ which best fits the observed star formation thresholds in external galaxies.

There is qualitative agreement between the region where the gas density lies above the predicted star formation threshold, $R \sim 4$–8 kpc, and the region of peak star formation as traced by the giant H II regions. At other radii, including the solar neighborhood, the gas lies below the predicted threshold density, and there we would expect the star formation to be restricted to perturbed regions, such as spiral arms. However, the same observations can be reproduced nearly as well by a simple Schmidt law (Güsten and Mezger 1983; Scoville and Good 1986), so the distribution of star formation in the Galaxy does not offer a clean test of the threshold model. Nevertheless, it is gratifying that the same star formation model which appears to describe external galaxies is also at least qualitatively consistent with the distribution of star formation in the Galaxy.

d) Radial Truncations of Stellar Disks

If the abrupt falloff in the SFR at the threshold radius persists for sufficient time, it should introduce a visible turnover or truncation of the observed stellar luminosity profile at that radius. Until recently such cutoffs in the stellar disks had not been reported, and this could pose a problem for the threshold model, at least in its simplest form. Recent work by van der Kruit (1988), however, suggests that many stellar disks may possess radial cutoffs at approximately the same location as seen in the star-forming regions. Outer edges are seen frequently in edge-on disks (van der Kruit 1979; van der Kruit and Searle 1981), and van der Kruit (1988) finds evidence for truncations in all but one of the 15 spirals (including face-on systems) in the survey of Wevers, Allen, and van der Kruit (1986). Unfortunately there is only one galaxy in our sample for which van der Kruit lists a cutoff radius (NGC 628); in that case the radii of the H II region and stellar disks are nearly identical. It would be extremely interesting to confirm the reality of these truncations in the stellar disks and to compare their radii with the predictions of the threshold model.

Van der Kruit (1989) has hypothesized that the stellar disk truncations are a direct consequence of the initial collapse and formation of the disk, following the general picture of Fall and Efstathiou (1980). In his scenario the cutoff radius is determined by the maximum angular momentum of the protogalactic halo. We hypothesize quite a different cause for the cutoffs, namely a cumulative effect over time of the gravitational threshold of the gas disk on the star formation. In late-type galaxies it may be possible to test this picture directly, by comparing the observed cutoff radii with the predictions of the threshold model (analogous to Fig. 12).

e) Suppression of Star Formation in S0 Galaxies

A considerable fraction of S0 and Sa galaxies possess large masses of interstellar gas but little or no detected star formation (Schommer and Bothun 1985; van Driel 1987; Thronson and Bally 1987), and such galaxies pose a clear problem for the standard Schmidt star formation model. The presence of a star formation threshold, however, provides a straightforward explanation for the low SFR in these systems. Although the
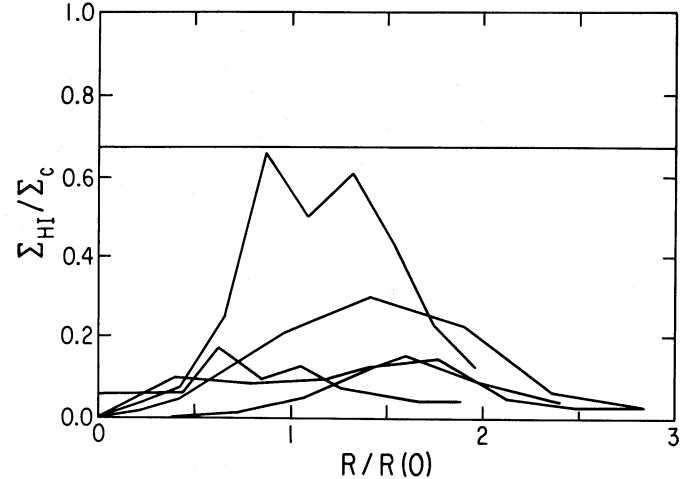

FIG. 17.—Radial behavior of the ratio of H I surface density to the critical density for gravitational stability, for five gas-rich S0 galaxies studied by van Driel. The radial coordinate is normalized to the isophotal radius of the disk. The horizontal line denotes the stability parameter $\alpha = 0.67$ which best fits the observed star formation thresholds in Sc galaxies.

integrated hydrogen masses of these red H I-rich galaxies are often comparable to those of late-type spirals, the surface density of gas in these sytems is quite often quite low, with $N(\text{H I}) < 10^{21}$ H cm^{-2}, or $\Sigma(\text{H I}) \ll 10\ M_\odot$ pc^{-2} (van Driel 1987; van der Hulst et al. 1987). These galaxies are often characterized by high rotation velocities as well, resulting in critical densities for gravitational stability which are usually much higher than the gas densities.

This point is illustrated in quantitative terms in Figure 17, which shows the radial behavior of the ratio of H I surface density to critical density (eq. [4]), for five S0 galaxies mapped by H I by van Driel (1987). Unfortunately CO maps are not yet available for these galaxies, but the H I distribution should at least be representative of the gas in the outer disks. The horizontal line in Figure 17 indicates the critical value $\alpha = 0.67$ which was derived for Sc galaxies. The S0 galaxies are characterized by H I disks which are below this threshold at all radii, and consequently the absence of active star formation in these galaxies is not surprising. CO observations are needed to verify that the total gas densities lie below the threshold, but in most cases the H I densities are so low (relative to the threshold) that the inclusion of molecular gas is not likely to alter our conclusions.

f) Starbursts in the Disks and Nuclei of Galaxies

Many interacting galaxies experience large bursts of star formation in their disks or nuclei, with increases in the SFR of 1–2 orders of magnitude (Larson and Tinsley 1978; Bushouse 1987; Kennicutt et al. 1987). Such bursts are difficult to explain if the SFR is a low power ($n = 1$–2) of the gas density, unless a strongly nonlinear process is introduced (e.g., Scalo and Struck-Marcell 1986). The star formation thresholds, however, provide a straightforward mechanism for producing starbursts in many types of galaxies. Our results show that the SFR is a very nonlinear function of density near the threshold limit, and if the gas disk of a galaxy were initially below the threshold at most radii, such as with most of the intermediate-type galaxies in Figure 13, even a modest perturbation of the disk could lead to very large increases in the global SFR. Struck-Marcell and

Scalo (1987) have reached similar conclusions, based on their models for interstellar cloud growth and star formation in disturbed galaxies.

As discussed earlier, the threshold density increases rapidly toward the center of a differentially rotating disk, so this mechanism could produce especially strong starbursts in the central regions of early-type galaxies. Critical densities in the central kiloparsec of rapidly rotating disks can easily reach surface densities of several hundred $M_\odot$ pc^{-2}, or volume densities of several hundred atoms cm^{-3}. Large concentrations of gas could accumulate in such an environment, and once the density did cross the threshold, star formation presumably would occur at a very high rate, corresponding to the high-density extrapolation of the star formation law (see Fig. 14).

g) Star Formation in Spiral Arms

The nonlinear increase in the SFR near the threshold density may also provide a straightforward explanation for the strong concentration of star formation in the spiral arms of many galaxies. In M51, for example, virtually all of the massive star formation occurs in the main pair of spiral arms, yet observations of the gas distribution by Rydbeck, Hjalmarson, and Rydbeck (1985) and Lord (1987) show that the gas density in the arms is enhanced by factors of only 1.2–2. A similar behavior is observed in the disk and spiral arms of NGC 6946 (Tacconi-Garman 1988). This is consistent with a Schmidt law for very large values of the power-law index ($n \gg 2$). However, comparison of the observed gas densities in these galaxies with the expected threshold densities suggests that the gas densities in the arm and interarm regions bracket the threshold value, and this may offer a simple explanation for the high arm-interarm contrast in the SFRs.

Our results may also provide an explanation for why the SFRs in galaxies with strong "grand design" spiral patterns are no higher on average than in galaxies which lack spiral structure (Elmegreen and Elmegreen 1986), a result which led Elmegreen and Elmegreen to question whether density waves trigger star formation. Our analysis suggests that the onset of active star formation is determined by the gravitational stability of the gas disk, independent of whether spiral structure is present. The critical condition for the development of spiral density waves, on the other hand, involves the gravitational stability of the stellar disk, following a condition similar to equation (4), but with the relevant parameters being the surface density and velocity dispersion of the stellar disk, rather than the gas. Our observations suggest that these two stability criteria are largely decoupled from one another; we see frequent examples of active star-forming galaxies with or without strong spiral structure, and conversely many examples of "grand-design" spirals which are essentially devoid of active star formation. In this sense the presence of spiral density waves does not appear in itself to be the predominant driver of the SFR, as pointed out by Elmegreen and Elmegreen (1986).

On the other hand, there are many examples of spirals where the average gas density appears to lie just below the threshold value (e.g., Fig. 13), and where spiral arms appear to have triggered most or all of the observed star formation. Many of these galaxies have relatively low integrated SFRs, but this is due to the low gas densities and the virtual absence of star formation between the arms, not to the lack of density wave triggered star formation. This effect may partly account for the tendency of the "grand design" spirals to have normal or even lower than average SFRs.

h) Problems and Future Work

The results in this paper appear to resolve many of the previous inconsistencies and problems with the standard Schmidt law picture of star formation in galaxies, but they have also left several important questions unanswered.

Although the radial behavior of the observed star formation in most galaxies is in qualitative accord with the threshold model, there are a few notable exceptions. Two nearby Sc galaxies, M33 and NGC 2403, possess active star formation throughout their inner disks, yet the gas densities in large portions of the disk lie well below the predicted threshold (see Fig. 11). In M33 the gas in the inner disk is heavily concentrated into spiral arms (Deul and van der Hulst 1987), and this might account for the apparent breakdown of the threshold model. Both galaxies also exhibit unusually weak CO emission, and we are tempted to speculate that in these systems the CO emission systematically underestimated the amount of molecular gas. Otherwise it is likely that some aspect of our simple threshold model does not apply to these galaxies.

Perhaps the most unsettling result of this investigation is the poor correlation between the observed SFRs and the molecular gas properties of the galaxies. This is not the first indication that the molecular gas is not as strong a tracer of the star formation as had been previously hoped; similar results have been discussed by Stark et al. (1986) and Kenney (1987). However, the virtual absence of any correlation between global Hα emission and CO emission found here is difficult to understand, and it is important to establish whether it is caused by a real decoupling between total molecular gas content and the SFR, or by problems with the Hα and/or CO emission as quantitative tracers of the SFR and molecular mass, respectively.

Our interpretation of the observed star formation law is incomplete in a number of respects. Our observations indicate that a Schmidt-type power law provides a reliable parametrization of the SFR for gas densities well above the threshold value, but they provide little insight into the physical basis of this law. Since our data are based on radial profiles of the SFR and gas density, we cannot separate a physical SFR–density relationship from a dependence of the SFR on metallicity, stellar disk density, or some other radially varying parameter. Our results may also be affected by radial gradients in either the extinction at Hα or the CO–H_2 conversion factor. Better constraints on the variations (if any) in these parameters would be very valuable.

The threshold picture presented here, essentially a reintroduction of the Quirk (1972) model, is certainly oversimplistic. We have adopted the simplest possible single-fluid gravitational stability model, and assumed a constant velocity dispersion for both cold gas components in all galaxies. It seems likely on phenomenological grounds that the scale height and velocity dispersion of the gas, and hence the stability threshold, are coupled to the SFR itself, and if this coupling is strong it will qualitatively modify the temporal behavior of the global SFR. Other potentially important factors, such as the cloud structure of the gas, magnetic fields, and cloud collision and growth time scales have not been considered at all. Nevertheless, our simple gravitational model appears to reproduce the basic features of observed star formation and gas distributions in most nearby disk galaxies.

Finally, it is important to reiterate that our results describe the regulation of the SFR on very large scales, and they provide little useful information on the local (<1 kpc) star

formation law. Analyses of the SFR on a point-by-point bias in selected galaxies will make it possible to test the threshold model and to define the limiting scales over which a global relation such as the Schmidt law is valid. This may make it possible to replace the Schmidt parametrization with a physical model for the large-scale star formation in galaxies.

REFERENCES

Berkhuijsen, E. M. 1977, *Astr. Ap.*, **57**, 9.
Bloemen, J. B. G. M., *et al.* 1986, *Astr. Ap.*, **154**, 25.
Bonnarel, F., Boulesteix, J., and Marcelin, M. 1986, *Astr. Ap. Suppl.*, **66**, 149.
Boroson, T. 1981, *Ap. J. Suppl.*, **46**, 177.
Bosma, A. 1981, *A.J.*, **86**, 1825.
Bosma, A., Goss, W. M., and Allen, R. J. 1981, *Astr. Ap.*, **93**, 106.
Buat, V., Deharveng, J. M., and Donas, J. 1989, *Astr. Ap.*, in press.
Burton, W. B. 1971, *Astr. Ap.*, **10**, 76.
Bushouse, H. A. 1987, *Ap. J.*, **320**, 49.
Clemens, D. P. 1985, *Ap. J.*, **295**, 422.
Cowie, L. L. 1981, *Ap. J.*, **245**, 66.
Davies, R. D., Elliott, K. H., and Meaburn, J. 1976, *Mem. R.A.S.*, **81**, 89.
DeGioia-Eastwood, K., Grasdalen, G. L., Strom, S. E., and Strom, K. M. 1984, *Ap. J.*, **278**, 564.
Deul, E. R., and van der Hulst, J. M. 1987, *Astr. Ap. Suppl.*, **67**, 509.
de Vaucouleurs, G., de Vaucouleurs, A., and Corwin, H. G. 1976, *Second Reference Catalog of Bright Galaxies* (Austin: University of Texas Press).
Donas, J., Deharveng, J. M., Laget, M., Milliard, B., and Huguenin, D. 1987, *Astr. Ap.*, **180**, 12.
Dopita, M. A. 1985, *Ap. J. (Letters)*, **295**, L5.
Elmegreen, B. G. 1979, *Ap. J.*, **231**, 372.
Elmegreen, B. G., and Elmegreen, D. M. 1986, *Ap. J.*, **311**, 554.
Fall, S. M., and Efstathiou, G. 1980, *M.N.R.A.S.*, **193**, 189.
Franco, J., and Cox, D. P. 1983, *Ap. J.*, **273**, 243.
Freedman, W. L. 1984, Ph.D. thesis, University of Toronto.
Garman, L., and Young, J. S. 1986, *Astr. Ap.*, **154**, 8.
Goldreich, P., and Lynden-Bell, D. 1965, *M.N.R.A.S.*, **130**, 97.
Guibert, J., Lequeux, J., and Viallefond, F. 1978, *Astr. Ap.*, **68**, 1.
Guideroni, B. 1987, *Astr. Ap.*, **172**, 27.
Guideroni, B., and Rocca-Volmerange, B. 1985, *Astr. Ap.*, **151**, 108.
Güsten, R., and Mezger, P. G. 1983, *Vistas Astr.*, **26**, 159.
Hodge, P. W. 1974, *Ap. J. Suppl.*, **27**, 113.
Hodge, P. W., and Kennicutt, R. C. 1983a, *A.J.*, **88**, 296.
———. 1983b, *Ap. J.*, **267**, 563.
———. 1983c, *An Atlas of* H II *Regions in 125 Galaxies* (PAPS Document ANJOA88-296-300).
Huchtmeier, W. K., and Witzel, A. 1979, *Astr. Ap.*, **74**, 138.
Hunter, D. A., and Gallagher, J. S. 1986, *Pub. A.S.P.*, **98**, 5.
Ikeuchi, S., Habe, A., and Tanaka, K. 1984, *M.N.R.A.S.*, **207**, 909.
Israel, F. P., and Kennicutt, R. C. 1980, *Ap. Letters*, **21**, 1.
Jog, C. J., and Solomon, P. M. 1984a, *Ap. J.*, **276**, 114.
———. 1984b, *Ap. J.*, **276**, 127.
Kenney, J. D. 1987, Ph.D. thesis, University of Massachusetts.
Kenney, J. D., and Young, J. S. 1988a, *Ap. J. Suppl.*, **66**, 261.
———. 1988b, *Ap. J.*, **326**, 588.
Kennicutt, R. C. 1983, *Ap. J.*, **272**, 54.
———. 1986, in *Stellar Populations*, ed. C. A. Norman, A. Renzini, and M. Tosi (Cambridge: Cambridge University Press), p. 125.
———. 1988, *Ap. J.*, in press.
Kennicutt, R. C., Edgar, B. K., and Hodge, P. W. 1989, *Ap. J.*, **337**, 761.
Kennicutt, R. C., Keel, W. C., van der Hulst, J. M., Hummel, E., and Roettiger, K. A. 1987, *A.J.*, **93**, 1011.
Kennicutt, R. C., Kent, S. M. 1983, *A.J.*, **88**, 1094.
Kulkarni, S. R., and Heiles, C. 1987, in *Interstellar Processes*, ed. D. J. Hollenbach and H. A. Thronson (Dordrecht: Reidel), p. 87.
Larson, R. B. 1983, *Highlights Astr.*, **6**, 191.
———. 1987, in *Starbursts and Galaxy Evolution*, ed. T. Montmerle and J. T. T. Van (Gif sur Yvette: Editions Frontieres), p. 467.
———. 1988, in *Galactic and Extragalactic Star Formation*, ed. R. E. Pudritz and M. Fich (Dordrecht: Reidel), p. 459.
Larson, R. B., and Tinsley, B. M. 1978, *Ap. J.*, **219**, 46.
Larson, R. B., Tinsley, B. M., and Caldwell, C. N. 1980, *Ap. J.*, **237**, 692.
Liszt, H. S., and Burton, W. B. 1983, in *Kinematics, Dynamics, and Structure of the Milky Way*, ed. W. L. H. Shuter (Dordrecht: Reidel), p. 135.
Lord, S. D. 1987, Ph.D. thesis, University of Massachusetts.
Madore, B. F. 1977, *M.N.R.A.S.*, **178**, 1.

Madore, B. F., van den Bergh, S., and Rogstad, D. H. 1974, *Ap. J.*, **191**, 317.
Maloney, P. R. 1987, Ph.D. thesis, University of Arizona.
McCall, M. L., Rybski, P. M., and Shields, G. A. 1985, *Ap. J. Suppl.*, **57**, 1.
Miller, G. E., and Scalo, J. M. 1979, *Ap. J. Suppl.*, **41**, 513.
Nakano, M., Ichikawa, T., Tanaka, Y. D., Nakai, N., and Sofue, Y. 1987, *Pub. Astr. Soc. Japan*, **39**, 57.
Newton, K. 1980, *M.N.R.A.S.*, **190**, 689.
Ohta, K., Sasaki, M., and Saito, M. 1988, *Pub. Astr. Soc. Japan*, **40**, 653.
Pompea, S. M., and Rieke, G. H. 1989, *Ap. J.*, in press.
Quirk, W. J. 1972, *Ap. J. (Letters)*, **176**, L9.
Quirk, W. J., and Tinsley, B. M. 1973, *Ap. J.*, **179**, 69.
Rogstad, D. H., and Shostak, G. S. 1972, *Ap. J.*, **176**, 315.
Rydbeck, G., Hjalmarson, A., and Rydbeck, O. E. H. 1985, *Astr. Ap.*, **144**, 282.
Sanders, D. B., Solomon, P. M., and Scoville, N. Z. 1984, *Ap. J.*, **276**, 182.
Scalo, J. M., and Struck-Marcell, C. 1986, *Ap. J.*, **301**, 77.
Schmidt, M. 1959, *Ap. J.*, **129**, 243.
Schommer, R. A., and Bothun, G. D. 1983, *A.J.*, **88**, 577.
Scoville, N. Z., and Good, J. C. 1986, in *Star Formation in Galaxies*, ed. C. J. Lonsdale Persson (NASA Conf. Pub. CP-2466), p. 3.
Scoville, N. Z., and Young, J. S. 1983, *Ap. J.*, **265**, 148.
Schweizer, F. 1976, *Ap. J. Suppl.*, **31**, 313.
Searle, L., Sargent, W. L. W., and Bagnuolo, W. G. 1973, *Ap. J.*, **179**, 427.
Shaya, E. J., and Federman, S. R. 1987, *Ap. J.*, **319**, 76.
Silk, J. 1987, in *Star Forming Regions*, ed. M. Peimbert and J. Jugaku (Dordrecht: Reidel), p. 663.
Skillman, E. D. 1987, in *Star Formation in Galaxies*, ed. C. J. Lonsdale Persson (NASA Conf. Pub. CP-2466), p. 263.
Solomon, P. M., Barrett, J., Sanders, D. B., and de Zafra, R. 1983, *Ap. J. (Letters)*, **266**, L103.
Stark, A. A. 1984, *Ap. J.*, **281**, 624.
Stark, A. A., Elmegreen, B. G., and Chance, D. 1987, *Ap. J.*, **322**, 64.
Stark, A. A., Knapp, G. R., Bally, J., Wilson, R. W., Penzias, A. A., and Rowe, H. E. 1986, *Ap. J.*, **310**, 660.
Struck-Marcell, C., and Scalo, J. M. 1987, *Ap. J. Suppl.*, **64**, 39.
Tacconi-Garman, L. J. 1988, Ph.D. thesis, University of Massachusetts.
Tacconi, L. J., and Young, J. S. 1986, *Ap. J.*, **308**, 600.
———. 1987, *Ap. J.*, **322**, 681.
Talbot, R. J. 1980, *Ap. J.*, **235**, 821.
Talbot, R. J., and Arnett, W. D. 1975, *Ap. J.*, **197**, 551.
Thronson, H. A., and Bally, J. 1987, *Ap. J. (Letters)*, **319**, L63.
Tinsley, B. M., and Danly, L. 1980, *Ap. J.*, **242**, 435.
Toomre, A. 1964, *Ap. J.*, **139**, 1217.
Twarog, B. A. 1980, *Ap. J.*, **242**, 242.
van der Hulst, J. M., Kennicutt, R. C., Crane, P. C., and Rots, A. H. 1988, *Astr. Ap.*, **195**, 38.
van der Hulst, J. M., Skillman, E. D., Kennicutt, R. C., and Bothun, G. D. 1987, *Astr. Ap.*, **177**, 63.
van der Kruit, P. C. 1979, *Astr. Ap. Suppl.*, **38**, 15.
———. 1988, *Astr. Ap.*, **192**, 117.
———. 1989, in *Le Monde des Galaxies*, ed. L. Bottinelli and H. G. Corwin, in press.
van der Kruit, P. C., and Searle, L. 1981, *Astr. Ap.*, **95**, 105.
van der Kruit, P. C., and Shostak, G. S. 1984, *Astr. Ap.*, **134**, 258.
van Driel, W. 1987, Ph.D. thesis, University of Groningen.
Verter, V. 1987, *Ap. J. Suppl.*, **65**, 555.
Warmels, R. H. 1986, Ph.D. thesis, University of Groningen.
———. 1988, *Astr. Ap. Suppl.*, **72**, 427.
Wevers, B. M. H. R., van der Kruit, P. C., and Allen, R. J. 1986, *Astr. Ap. Suppl.*, **66**, 505.
Wyse, R. F. G. 1986, *Ap. J. (Letters)*, **311**, L41.
Young, J. S. 1987, in *Star Formation in Galaxies*, ed. C. J. Lonsdale Persson (Washington: NASA Conf. Pub. CP-2466), p. 197.
Young, J. S., and Scoville, N. 1982a, *Ap. J.*, **258**, 467.
———. 1982b, *Ap. J. (Letters)*, **260**, L11.
———. 1982c, *Ap. J. (Letters)*, **260**, L41.
Young, J. S., Scoville, N. Z., and Brady, E. 1985, *Ap. J.*, **288**, 487.

ROBERT C. KENNICUTT, JR: Steward Observatory, University of Arizona, Tucson, AZ   85721